

1 New insight on tide-dominated estuary and delta in the Eocene-
2 Miocene Mrayt Group, North-Western Rif, Morocco

3
4 Choukri Chacrone¹, Naima Hamoumi², Silvia Spezzaferri³

5
6 ¹Centre régional des métiers de l'éducation et de la Formation (CRMEF) de Casablanca Hay Hassani, Maroc

7 ²Research group ODYSSEE, Department of Earth Sciences, Mohammed V University, Rabat, Morocco

8 ³Université de Fribourg, Department of Geosciences, Earth Sciences, 1700 Fribourg, Switzerland



Choukri Chacrone

11 choukrichacrone@gmail.com

12
13
14
15
16
17
18
19
20
21
22 This manuscript is a non-peer reviewed EarthArXiv preprint, and has been
23 submitted for publication in Arabian Journal of Geosciences.

1 Abstract

2 The sedimentary deposits of Eocene-Miocene Mrayt Group, North-Western Rif, Morocco has been the subject of
3 controversy by previous works regarding their depositional environments. Detailed sedimentological study based
4 on petrographic study, and sedimentary facies and paleocurrent measurements analysis, leads to several results
5 and new insights.

6 Petrographic study provided the first evidence of mixed siliciclastic and carbonate sediments and their
7 nomenclature: silty micrites, micritic siltstones, micritic sandstones, sandy micrite, and allochemic sandstones, as
8 well as the nature of the sediment sources and their geological context.

9 Twenty two sedimentary facies that have never been described before are identified, and based on their
10 succession and association a new interpretation of depositional processes and depositional systems are proposed.
11 The paleoenvironments of the Mrayt Group are interpreted as littoral and shallow marine settings: tides-
12 dominated estuary, tides-dominated delta systems and open coast tidal flat, under complex hydrodynamics
13 strongly influenced by river discharge, tidal currents, waves and storms action.

14 Sedimentation occurred in “the Maghrebian basin” under the interplay of: i) tectonics related to the Cenozoic
15 collision of the African and Eurasian continental plates, ii) Cenozoic alternation of warm climate and cooling
16 due to the increasing influence of Antarctica glaciation, iii) sediments supplies induced by rejuvenation of
17 sedimentary sources and iv) sea level fluctuation related to the advance and retreat of ice-sheet on Antarctica.

18

19 **Key words** Tide dominated delta, mixed siliciclastic/carbonate rocks, Mrayt Group, NW Rif, Morocco, Eocene
20 –Miocene

21

22 Introduction

23

24 The alpine Rif belt has been studied since 1846 in the frame of several national and international programs. Most
25 of these researches focused on tectonic, geochemistry, petrography, biostratigraphy and geophysics, while
26 sedimentology was mostly neglected. Thus, the paleogeography and the geology of the region reported in
27 geological maps of the NW Rif sections were interpreted without taking into account the sedimentary facies and
28 their variations. This has given origin, to the many controversies on the relationships between the tectono-
29 paleogeographic units, and their lithostratigraphy (Hamoumi 1995a). The paleogeography in this area is complex

1 and mostly unconstrained, therefore, sedimentological facies and depositional environmental analysis is
2 important to reconstruct this.

3 Sedimentological studies conducted in the flysch domain of the NW Rif belt, in the framework of “The
4 Linked Project Cross the Strait of Gibraltar between Africa and Europe” (Hamoumi 1995b; Hamoumi et al.
5 1995; Ouldchelha et al. 1995; Salhi et al. 1995), has highly contributed to the knowledge of the depositional
6 environments that prevailed over the Cretaceous-Miocene period and their allogenic and autogenic control.
7 The Eocene-Miocene Mrayt Group, in the North Western Rif, Morocco was described for the first time by Suter
8 and Fiechter (1966) and called “Flysch de Sidi Mrayt” by Suter (1986). It has been studied for its tectonics,
9 lithostratigraphy, biostratigraphy and sedimentology (Suter and Fiechter 1966; Suter 1980; Suter 1986; Morley
10 1992; Tejera of Leon 1993; Abdelkhaliki 1997; Raissouni et al. 2008). Although these studies have agreed on the
11 lithostratigraphic characteristics of these sedimentary series, there are, however, discrepancies concerning the
12 environment in which they were deposited. Indeed, the deposits of this group have been interpreted as: 1)
13 synorogenic turbidites organized in two sequences (Morley 1992): a lower sequence referred to a Type I deep
14 sea fan system, and an upper sequence linked to a Type III deep sea fan system (sensu Mutti 1985); 2) reworked
15 and redeposited slope sediments by bottom currents on an abyssal plain, capped by slides and mass flow deposits
16 that accumulate at the end of slope in un-channelized areas (Tejera de Leon 1993); 3) a sedimentary prism
17 adjacent to the outer edge of the platform subjected to storm waves action and passing to a Mutti type III deep
18 sea fan system (Raissouni et al. 2008).

19 Detailed sedimentological study conducted for the first time in the Mrayt Group, allows bringing new
20 results concerning: the nature of the sediments and their sources, the sedimentary facies, the depositional systems,
21 the sedimentary processes and the allogenic control. The aims of this work are: 1) to highlight the mixed
22 composition (siliciclastic/carbonate) of the Mrayt Group sediments and to introduce a more adequate
23 nomenclature for these deposits; 2) to bring new findings, including the characterization of new sedimentary
24 facies never described before and a new interpretation of the depositional processes and sedimentary
25 environments corresponding to tide-dominated estuary, tide-dominated delta systems and open-coast tidal flat; 3)
26 to document the evolution from tide-dominated estuary to tide-dominated delta and then to open-coast tidal
27 flat and its control during the Eocene–Miocene in the Rif alpine belt.

28 In addition to these new results this study is important for increasing our knowledge about ancient tide-
29 dominated delta that is less investigated in comparison to the other deltaic systems (waves or river dominated)
30 and its responses to sea level changes and tectonics. Tide-dominated deltas are those where tide currents are the

1 dominant process controlling sediment dispersal (Galloway 1975; Goodbread and Saito 2012, and references
2 therein). Furthermore correct interpretation of Eocene–Miocene sedimentary sections of the North Western Rif is
3 essential to understand the paleogeography and the geodynamic evolution of the Rif alpine belt which is a part of
4 the peri Mediterranean alpine belt. It's also critical for regional economies as deltas may contain significant
5 volumes of oil and gaz.

6

7 Geological setting

8

9 The Mrayt Group is a 1730 m-thick sedimentary unit crops out in the North Western Rif along the Atlantic
10 littoral between the cities of Asilah and Larache in North Morocco (Fig. 1). It belongs to the Prerif domain of the
11 Rif belt (Suter and Fiechter 1966). The Rif belt represents the westernmost part of the Maghrebide belt that
12 belongs to the western part of the alpine Mediterranean orogen and its connected to the Betic belt through the
13 Gibraltar arc (Fig. 1A). It corresponds to a syntectonic province characterized by the alpine folding related to the
14 Tertiary collision between Alboran microplate, the Iberian plate and the African from the Oligocene to the Late
15 Miocene (9-8 Ma) (Dewey et al. 1989; Srivastava et al. 1990; Leprêtre et al. 2018 and references therein).

16 The Rif belt (Fig. 1B) is composed of three main structural units, from West to East: i) the “external Zone”
17 that consists of three stacked units (in ascending order): the Prerif, the Mesorif and the Intrarif, ii) the flysch
18 thrust sheets composed of several tectonic units as the Numidian flyschs, the Mauritanian flyschs and the
19 Merinide flyschs and iii) the “internal Zone” considered as a part of the “Thetysian Alboran Terrane” (Durand-
20 Delga et al. 1962; Andrieux 1971; Suter 1980).

21 The Mrayt Group (Fig. 1B and Fig. 1C) crops out in the North western “external Zone” of the Rif North of
22 the Jebha-Chrafat accident and is overlapped to the East by the allochthonous Habt unit (Suter 1980 and 1986).
23 It's deformed by a section of anticline and syncline folds trending S-N, and separated by overthrust faults (Tejera
24 de Leon 1993). Stratigraphically, the Mrayt Group rests on Cretaceous marlstones and consists of four
25 Formations (Tabl. 1) from base to top: Lower pelitic” formation, Sandstone-pelitic formation, Upper sandstone-
26 pelitic formation and Si Moussa Formation which rests unconformably on the underlying formation. These
27 formations are ranging in age from the Lower Eocene to the Middle Miocene based on microfossils (Suter and
28 Fiechter 1966; Suter 1980 and 1986; and Tejera de Leon 1993).

29

1 **Tabl. 1** Lithostratigraphy of the Mrayt Group formations (after Suter and Fiechter 1966; Suter 1980 and 1986; and
 2 Tejera de Leon 1993)

Formation		Thickness	Lithology	Age
Si Moussa Formation		500m	Interbedded sandstones and marly pelites	Middle Miocene (Langhian)
Upper pelitic Formation		100m	Interbedded sandstones and pelites	Upper Oligocene to Lower Miocene
Sandstone and pelitic Formation	Upper conglomeratic member	400m	Interbedded sandstones, pelites and conglomerates	Early to Upper Oligocene
	Lower sandstones and pelitic member	600m	Interbedded sandstones, pelites and microglomerates	
Lower pelitic Formation	Upper member	100m	Interbedded sandstones and pelites	Lower Eocene
	Lower member	50m	Interbedded microglomerats, sandstones and marlstones	

3

4 Methods

5

6 Reconstruction of Mghait Group depositional environments is based on analysis and interpretation of
 7 sedimentary facies and sedimentary facies associations as well as paleocurrent measurements. Sedimentary
 8 facies are identified on the basis of their petrofacies and lithofacies. The petrofacies is here defined in term of
 9 composition and texture introduced for rocks classification (Mansfield 1971; Dickinson and Rich 1972). The
 10 lithofacies refers to a body of rock with specific characteristics that form under certain conditions of
 11 sedimentation, reflecting a particular process or environment. It's defined on the basis of lithology, colour,
 12 bedding (thickness, geometry, nature of the contacts separating the strata, internal architecture) and physical and
 13 biological sedimentary structures (see references in Reineck and Singh 1980; Reading 1986; Walker 1992).

14 Five sections belonging to the Mrayt Group, totalizing 1730 m thickness has been subjected to detailed
 15 sedimentological study including sampling (Fig. 1C). They are named: MG1- Damina section, 80m thick (X=
 16 6.06; Y= 35.42), MG2- Marabout section, 750m thick (X= 5.85; Y= 35.36), MG3- Sidi Mrayt beach section,

1 200m thick (X= 5.85; Y= 35.41), MG4- Merja section, 520m thick (X= 5.96; Y= 35.43), and MG5- Merja ravine
2 section, 280m thick (X= 6.05; Y= 35.44).The stratigraphic sections were logged in a high detail using bed by bed
3 centimeter-scale description of: lithology, colour, bedding (thickness, geometry, nature of the contacts
4 separating the strata and internal architecture) and physical and biological sedimentary structures.

5 The petrographic study has been based on the examination of 50 thin sections under polarizing microscope.The
6 determination of the composition takes into account the detrital, authigenic and organic constituents and the
7 texture includes the proportion of clay matrixand the shape, roundness, surface features, grain sizeand fabric of
8 the grains. The petrographic study, indicate that the investigated sedimentary rocks are composed of mixtures of
9 siliciclastic and carbonate sediments. The existence of carbonates had already been demonstrated by the reaction
10 to HCL during the fieldwork. Therefore it was necessary to apply the classification of Mount (1985) in order to
11 establish the precise nomenclature for the petrofacies. This classification defined eight general classes of mixed
12 sediments based on the percentage of the four components: i) siliciclastic sand (sand-sized quartz, feldspar, etc.),
13 ii) mud (mixtures of silt and clay), iii) allochems (carbonate grains such as peloids, ooids, bioclasts and
14 intraclasts > 20pm in size) and iv) carbonate mud or micrite (< 20 pm in size). The name of the class is based on
15 both dominant grain type and the most abundant antithetic components. For example a sedimentary rock that
16 contain more than 50% sand-sized siliciclastic components and accessory allochems,is named an allochemic
17 sandstone.

18 In each section, the sedimentary facies identified were clustered into sedimentary facies association (Reading
19 1986)according to the following criteria: their environmental significance, their genetic relationship and their
20 situation in relation to each otheraccording to Collinson (1969) and Reading (1986). The paleocurrent
21 measurements were performed on 48 flute casts in the five studied stratigraphic sectionsand the dip of longest
22 axis of the clasts in the three conglomerate levels (Facies F17).

23

24 Sedimentary facies analysis

25

26 The Petrofacies

27 The Petrographical analysis show that the Mrayt Group deposits consist of mixed siliciclastic / carbonate
28 sediments, composed of: siliciclastic and carbonate grains, matrix and cement (Fig. 2). The siliciclastic minerals
29 consists of: 1) moderately sorted, angular, sub-rounded or rounded detrital quartz grains, that may be

1 monocrystalline with undulating extinction or polycrystalline (polygonised quartz, slightly sutured grains and
2 chert) and sometimes with a secondary quartz overgrowths; 2) sub-rounded to sub-angular, < 0.125 mm in size
3 feldspar grains (microcline, plagioclase and orthoses) which are affected by alteration to various degrees ; 3)
4 sub-rounded to angular, > 2 µm in size lithic clasts of sedimentary, volcanic or metamorphic origin,; 4) altered
5 micas (muscovite, biotite and chlorite); 5) glauconitic grains; 6) heavy minerals (rounded zircons, green
6 tourmaline) and 7) opaque minerals including iron oxides. Carbonate components consist of: calcite lithoclasts
7 which may include benthic and planktonic foraminifera including e.g., Orbitolina and sometimes micritized
8 Calpionella, skeletal fragments of: gastropods, bivalves, echinoderms, bryozoans and algae and sometimes
9 rhombohedral crystals of dolomite. The bonding phase is composed of carbonate cement (microsparite and
10 sparite), ferruginous and siliceous cements, and sometimes by a clay matrix. Five petrofacies were identified
11 based on the percentage of the dominant grain type and the most abundant antithetic components, according to
12 Mount (1985) classification. These petrofacies are: silty micrites, micritic siltstones, micritic sandstones, sandy
13 micrites, and allochemic sandstones (Fig. 2, photos A, B, C and D).

14

15 The Sedimentary Facies

16 Sedimentological field studies combined with petrofacies analysis have resulted in the recognition for the first
17 time of twenty two sedimentary facies, in the five studied outcrops of the Mrayt Group (Fig. 3, 4, 5, 6, 7 and 12).

18 Facies F1 (Fig. 3A and Fig. 6), is observed in the lower Pelitic Formation of Early to Middle Eocene age
19 (Fig. 3). It consists of alternating centimetric to decimetric micritic siltstone bed and decimetric bioturbated marl
20 interbed. The bed has an undulating, erosive lower base and generally contains five intervals (from base to top): 1)
21 an interval (a) limited to its top by a reactivation surface and made up of successive couplets of thick (1-5cm) and
22 thin (0.5-1cm) planar parallel micritic siltstone laminae limited each one to its upper surface by very thin mud
23 layers (mm-scale) or mud drapes, 2) an interval (b) composed of ripple-cross-stratified micritic siltstone and mud
24 layers slightly following the concavity and convexity of the underlying rippled surface, 3) an interval (c) with
25 alternating planar parallel laminae of silty micrite and mud drapes, 4) an interval (d) composed of ripple-cross-
26 laminated micritic siltstone which displays symmetrical and asymmetrical ripples in which small lenses of mud
27 are preserved in the trough of the ripple and 5) an interval (e) composed of micritic siltstone with ripples that vary
28 in size and shape in the same layer. The top of bed shows centimetric to decimetric-scale desiccation cracks.

29 Facies F2 (Fig. 3B and Fig. 6), occurs in the lower Pelitic Formation of Early to Middle Eocene age (Fig. 3). It
30 consists of alternating centimetric to decimetric micritic siltstone bed and decimetric bioturbated marl interbed.

1 The bed is erosively based and displays three intervals (from base to top): 1) an interval (a) composed of ripple-
2 cross-laminated micritic siltstone which displays symmetrical and asymmetrical ripples in which small lenses of
3 mud are preserved in the trough of the ripples, 2) an interval (b) composed of ripple-cross-stratified micritic
4 siltstone and mud layers, slightly following the concavity and convexity of the underlying rippled surface, and 3)
5 an interval (c) composed of rippled micritic siltstone lenses on a muddy layer. The top of the bed shows *Zoophycos*
6 trace fossil, *Psilonichus* Y-shaped burrows and centimetric to decimetric-scale desiccation cracks.

7 Facies F3 (Fig. 3C and Fig. 6), is identified in the lower Pelitic Formation of Early to Middle Eocene age
8 and the upper part of the Sandstone and pelitic Formation of Upper Oligocene age (Fig. 3). It consists of lenticular,
9 cm-thick sandy micrite layer, intercalated with metric pelitic level. The sandy micrite bed is erosively based and
10 is composed of two intervals. The lower interval (a) is slightly deformed, without visible bedding and the upper
11 interval (b) is characterized by asymmetrical ripples which may display two types of internal structures: 1)
12 offshooting and draping laminations expressed by forest laminae which ascend and overlap the flank of the
13 adjoining ripple, 2) composite internal structure made up of an assemblage of differently structured, generally
14 bidirectional lenses. The top of this interval contains straight-crested ripples and sometimes contains *Zoophycos*
15 trace fossil, *Psilonichus* Y-shaped burrows and centimetric to decimetric-scale desiccation cracks.

16 Facies F4 (Fig. 3D and Fig. 6), occurs in the lower Pelitic Formation of Early to Middle Eocene age and the
17 upper part of the Sandstone and pelitic Formation of Upper Oligocene age (Fig. 3). It consists of centimeter to
18 decimetric lenticular sandy micrite bed intercalated with metric pelitic level. The bed has an erosively undulating
19 base and an erosive top. It is composed of two intervals: the basal interval (a) comprises sets of parallel plane
20 laminae, separated by reactivation surfaces. The upper interval (b) consists of tangential cross-laminated cm-
21 bundles separated by erosional surface and mud drape. The top of this interval exhibits centimetric to decimetric
22 desiccation cracks.

23 Facies F5 (Fig. 3E and Fig. 6), is identified in the lower Pelitic Formation of Early to Middle Eocene age
24 (Fig. 3). It consists of interbedded centimeter to decimetric silty micrite bed and decimetric bioturbated pelitic
25 layer. The silty micrite bed has an erosive undulating base and is generally composed of 3 intervals: 1) a lower
26 interval (a) exhibiting mud pebbles and asymmetric ripples characterized by a planar base and planar cross-
27 lamination, 2) a structureless intermediate interval (b), and 3) an upper interval (c), characterized by parallel
28 undulated laminations, pinching and swelling laterally and passing to incipient lenses. The top of the upper
29 interval is characterized by linguoid ripples and may show centimetric to decimetric desiccation cracks.

1 Facies F6 (Fig. 3F and Fig. 6) occurs in the lower Pelitic Formation of Early to Middle Eocene age (Fig. 3). It
2 consists of alternating centimeter to decimetric silty micrite bed and decimetric bioturbated pelitic interbed. The
3 bed is erosively based and comprises four intervals. The first interval (a) displays stacked sequences separated
4 from each other by mud drapes, each sequence is composed of a set of thick laminae, which thin progressively
5 from the bottom to the top. The second interval (b) is characterized by asymmetrical ripples displaying
6 offshooting and draping laminations expressed by foreset laminae which ascend and overlap the flank of the
7 adjoining ripple. The third interval is similar to the first one and the fourth interval is similar to the second one.
8 The top of the bed exhibits straight-crested ripples.

9 Facies F7 (Fig. 3G and Fig. 6), is documented in the lower Pelitic Formation of Early to Middle Eocene age
10 (Fig. 3). It consists of alternating centimeter to decimeter-thick micritic siltstone bed containing thin mud layers or
11 mud drapes and decimetric bioturbated pelitic interbed. The bed has undulating erosive base and it's composed
12 of 2 intervals. The lower interval (a) consists of stacked microsequences separated from each other by a
13 reactivation surface. Each microsequence displays successive couplets composed of thick (1-5cm) and thin (0, 5-
14 1cm) planar parallel micritic siltstone laminae limited each one to its upper surface by very thin mud layers (mm-
15 scale). The individual couplet thickness thin and thicken progressively from the bottom to the top of the
16 microsequence. The upper interval (b) displays sigmoid-shaped sets separated by reactivation surface or mud
17 drape and made up of successive couplets composed of thick (1-5cm) and thin (0,5-1cm) sigmoidal oblique
18 micritic siltstone laminae limited each one to its upper surface by very thin mud layers (mm-scale). The upper
19 surface of this interval contains centimetric to decimetric-scale desiccation cracks.

20 Facies F8 (Fig. 4A and Fig. 6), is identified in the lower Sandstone and pelitic Formation of Lower to Upper
21 Oligocene age (Fig. 3). It corresponds to an alternation of centimetric silty micrite bed and metric pelitic interbed.
22 The bed displays planar parallel laminations or tabular cross-laminations that may be disturbed by convolute
23 bedding. Its basal bounding surface is erosive and highly bioturbated, it sometimes shows Paleodictyon and
24 Cruzian trace fossils.

25 Facies F9 (Fig. 4B and Fig. 6), is documented in the lower Sandstone and pelitic Formation of Lower to
26 Upper Oligocene age (Fig. 3). It consists of alternating cm- to dm-thick sandy micrite bed and bioturbated pelitic
27 dm-thick interbed. The bed is lenticular with tangential cross laminations and an erosive base exhibiting
28 Paleodictyon and Cruzian trace fossils, grooves casts, prod casts and bounce casts. The upper surface of the bed
29 contains centimeter to decimetric desiccation cracks.

1 Facies F10 (Fig. 4C and Fig. 6), occurs in the lower Sandstone and pelitic Formation of Lower to Upper
2 Oligocene age (Fig.3).It consists of alternating decimetric pelitic interbed and centimetric to decimetric sandy
3 micrite bed composed of 4 intervals (a,b,c and d from base to top), separated by erosional surface and mud drape.
4 The first interval(a)exhibits an erosive base with groove casts, prod casts, flute casts and Ophiomorpha burrows,
5 and stacked microsequences separated from each other by a mud drape. Each microsequence displays successive
6 couplets of thick (1-5cm) and thin (0, 5-1cm) planar parallel micritic siltstone laminae limited each one to its
7 upper surface by very thin mud layers (mm-scale). The individual couplet thickness thins progressively from the
8 bottom to the top of the microsequence. The second interval (b) is cross laminated characterized by asymmetrical
9 ripples displaying various internal structures: 1) offshooting and draping laminations expressed by inclined
10 foreset laminations passing the trough and ascending onto the flank of the adjacent ripple, 2) composite internal
11 structure, made up of an assemblage of differently structured, generally multidirectional lenses, 3) swollen lens-
12 like sets, and 4) undulating parallel laminations passing into cross laminations, The third interval (c) shows an
13 undulating highly erosive lower bounding surface and it is fully disturbed by flame and convolute structures. The
14 fourth interval is similar to the first one, and displays in its upper surface symmetrical ripples and mud pebbles.

15 Facies F11 (Fig. 4D and Fig. 6), is observed in the lower Sandstone and pelitic Formation of Lower to Upper
16 Oligocene age (Fig.3). It is composed of alternating decimetric lenticular allochemic sandstone bed, and
17 decimetric pelitic interbed. The bed is erosively based with groove casts, prod casts, bounce casts and flute casts
18 may display convolute bedding, and it contains 3 intervals separated by reactivation surfaces. The lower interval
19 (a) shows interbedded rippled sandy layers and continuous mud drapes overlapping the ripple troughs and
20 crests. The intermediate interval (b) is a laminated sandy bed displaying sigmoidal cross laminations, successive
21 foreset laminations directed in opposite directions in superimposed layers and reactivation surfaces. The upper
22 interval (c) exhibits stacked microsequences separated from each other by mud drape. Each microsequence
23 displays successive couplets composed of thick (1-5cm) and thin (0, 5-1cm) planar parallel micritic siltstone
24 laminae limited each one to its upper surface by very thin mud layers (mm-scale). The individual couplet
25 thicknesses thicken progressively from the bottom to the top of the microsequence. The upper surface of this
26 interval is erosive and may show decimetric-scale desiccation cracks and mud pebbles.

27 Facies F12 (Fig.4E and Fig. 6), occur in the lower Sandstone and pelitic Formation of Lower to Upper
28 Oligocene age (Fig.3).It consists of alternating centimeter to decimetric silty micrite bed containing thin mud
29 layers or mud drapes and decimetric bioturbated pelitic interbed. The bed is erosively based with groove and flute
30 casts, and comprises four intervals (a, b, c and d from base to top), separated by erosional surface and/or mud

1 drape. The first interval (a) is composed of asymmetrical ripples characterized by lateral variation in size and
2 shape in the same layer and irregular, undulating lower bounding surface, which may be disturbed by convolute
3 bedding. The second interval (b) is made up of stacked microsequences separated from each other by a
4 reactivation surface. Each microsequence displays successive couplets composed of thick (1-5cm) and thin (0.5-
5 1cm) planar parallel micritic siltstone laminae, limited each one to its upper surface by very thin mud layers
6 (mm-scale). The individual couplet thickness thins progressively from the bottom to the top of the microsequence.
7 The third interval (c) is characterized by: 1) asymmetrical ripples displaying offshooting and draping laminations
8 expressed by foreset laminae which ascend and overlap the flank of the adjoining ripple and 2) ripples displaying
9 unidirectional cross lamina concordant with the lee side and laying on the same planar base. The fourth (d)
10 interval exhibits tangential cross laminated cm-bundles, separated by erosional surfaces and mud drapes.

11 Facies F13 (Fig. 4F and 4G, and Fig. 6), occurs in the lower Sandstone and pelitic Formation of Lower to
12 Upper Oligocene age (Fig. 3). It consists of alternating decimetric muddy layer and amalgamated decimetric,
13 lenticular coarse-micritic sandstone bed. The bed has an erosively undulating base and an erosive top exhibiting
14 metric scale wavelength hummocks, centimetric to decimetric desiccation cracks and soft pebbles. Its internal
15 structure shows hummocky cross stratification expressed by successive lamina sets separated by low angle
16 truncation surface and composed of parallel low-angle curved lamina which dome upward (hummocks) passing
17 laterally into laminae that are concave upward (swaley).

18 Facies F14 (Fig. 4H and Fig. 6), is observed in the lower Sandstone and pelitic Formation of Lower to Upper
19 Oligocene age (Fig. 3). It consists of interbedded, centimeter -to -decimeter -scale microconglomeratic bed with
20 rich in organic matter and strongly bioturbated plurimetric pelitic layer. The bed has a lenticular shape and an
21 erosive base with flute casts. It's made up of a fining upward microconglomerate containing rock clasts and shell
22 fragments.

23 Facies F15 (Fig. 4I and Fig. 6), occur in the lower Sandstone and pelitic Formation of Lower to Upper
24 Oligocene age (Fig. 3). It consists of alternation of decimetric pelitic layer and decimetric sequence of coarse-
25 grained sediments. The sequence has an erosive base exhibiting flute casts and it is composed of 6 intervals
26 (from base to top): 1) a lenticular metric fining upward microconglomerate containing rock clasts and shell
27 fragments (a); 2) a massive allochemic sandstones with dish pillar structures and convolute bedding (b);
28 3) ripple- cross-laminated micritic siltstone displaying unidirectional cross lamina concordant with the stoss
29 side (c); 4) couplets of thick (1-5cm) and thin (0.5-1cm) planar parallel micritic siltstone laminae limited each one to
30 its upper surface by very thin mud layers (mm-scale) separated sometime by reactivation surface (d); 5) micritic

1 siltstone interval bounded by reactivation surfaces and exhibiting sigmoidal cross laminated bundle (e) and (f) and (g)
2 micritic siltstone bed with asymmetrical ripples in which small lenses of mud are preserved in the trough of the
3 ripple (f). The top of the sequence shows mud pebbles and Ophiomorpha and Skolithos burrows.

4 Facies F16 (Fig. 4J and Fig. 6), is documented in the lower Sandstone and pelitic Formation of Lower to
5 Upper Oligocene age (Fig. 3). It consists of an alternation of decimetric pelitic layer and decimetric sequence of
6 coarse-grained sediments. The sequence has an erosive base exhibiting flute casts and it's made up of 3 intervals.
7 The lower interval (a) is a lenticular fining upward microconglomerate with rock clasts and shell fragments,
8 displaying tangential cross-stratification, which pass upward into sandy micrite disturbed by convoluted bedding.
9 The intermediate interval (b) is an allochemic sandstones composed of stacked microsequences separated from
10 each other by a mud drape. Each microsequence display successive couplets composed of thick (1-5cm) and thin
11 (0, 5-1cm) planar parallel micritic siltstone laminae limited each one to its upper surface by very thin mud layers
12 (mm-scale). The individual couplet thickness thin and thicken progressively from the bottom to the top of the
13 microsequence. The upper interval (c) is an erosively based and cross-stratified silty micrite displaying bundle of
14 sigmoidal laminae separated by mud drapes and reactivation surfaces. The top of this sequence shows
15 Zoophycos, and Ophiomorpha trace fossils.

16 Facies F17 occurs in the upper part of the lower Sandstone and pelitic Formation of Upper Oligocene age
17 (Fig. 3); it can be divided into three subfacies: F17a, F17b and F17c subfacies. F17a (Fig. 4K and Fig. 6) is a
18 reddish brown lenticular coarse bed with sharp base ranging in thickness from 4 to 5m. It consists of a matrix-
19 supported conglomerate, structureless, ungraded and without any preferred clast imbrication/organization. The
20 clasts consist of pelite, marlstone, sandstone, carbonate, granite and basalt. They are well rounded, angular or
21 elongated and poorly sorted, they range from 2 cm to 90 cm in length. The matrix is poorly sorted it's composed
22 of fine grained gravels, fine to very coarse grained sand, mud and carbonate cement. Subfacies F17b (Fig. 4K and
23 Fig. 6) is a decimetric brownish yellow medium to fine -grained sandstone bed with erosional base and flat top,
24 displaying planar cross stratification with some horizontal laminations and ripples. Subfacies F17c (Fig. 4L and
25 Fig. 6), consists of a lenticular reddish brown, coarse-grained unit composed of two intervals. The lower interval
26 (b) is a high erosively based clast-supported conglomerate bed ranging in thickness from 2 to 3 m. The clasts
27 consist of pelite, marlstone, sandstone, carbonate, granite and basalt. They are well rounded to angular and poorly
28 sorted, they range from 2 cm to 25 cm in length and they display ENE - WSW AB-plane type. The matrix is
29 composed of fine to very coarse grained sand, fine grained gravels, bivalve shells debris, and occasionally
30 carbonates cement. The upper interval is an erosively based decimetric allochemic sandstone unit which fines

1 upward to very fine-grained sandstones and exhibits planar and through cross-stratified beds separated by
2 erosional surfaces.

3 Facies F18 (Fig. 5A,5B, and Fig. 6), is observed in the upper part of the upper Sandstone and pelitic
4 Formation of Upper Oligocene to the Lower Miocene age (Fig.3). It consists of alternating metric coarse-sandy
5 micrite bed and decimetric to metric highly bioturbated muddy layer. The bed has an erosively undulating base
6 with load cast, and an erosive top. It's composed of low-angle cross laminated sets separated by erosional
7 surfaces and displays Ophiomorpha burrows, convolutes bedding, slumps and ball and pillow.

8 Facies F19 (Fig. 5C and Fig. 6), is identified in the upper part of the upper Sandstone and pelitic Formation
9 of Upper Oligocene to the Lower Miocene age (Fig.3). It consists of alternating metric coarse-sandy micrite bed
10 and decimetric to metric highly bioturbated muddy layer. The bed has an erosively undulating base with load
11 casts, and an erosive top and it's composed of stacked planar, quasi planar laminated tabular sets separated by
12 reactivation surface or mud drape. The bedding may be disturbed by convolutes bedding and water escape
13 structures.

14 Facies F20 (Fig. 5D and Fig. 6), occurs in the upper part of the upper Sandstone and pelitic Formation of
15 Upper Oligocene to the Lower Miocene age (Fig.3). It consists of alternating metric coarse-sandy micrite bed and
16 decimetric to metric highly bioturbated muddy layer. The bed is erosively based with load casts and its upper
17 surface is sharp and may display decimeter scale wavelength hummocks or ripples. Its internal structure shows
18 sets of planar parallel lamina passing to micro-hummocky cross stratification expressed by successive lamina
19 sets separated by low angle truncations surface and composed of parallel low-angle curved lamina which dome
20 upward (hummocks) passing laterally into laminae that are concave upward (swaley).

21 Facies F21 (Fig. 5E and Fig. 6), is documented in the upper part of the upper Sandstone and pelitic
22 Formation of Upper Oligocene to the Lower Miocene age (Fig.3). It consists of alternating metric coarse-sandy
23 micrite bed and decimetric to metric highly bioturbated muddy layer. The bed has an undulated erosive lower
24 base with load casts, and generally contain 3 intervals (a, b and c from base to top). The lower interval (a)
25 is limited to its top by an erosional surface and made up of successive couplets of thick (1-5cm) and thin (0.5-
26 1cm) planar parallel micritic siltstone laminae limited each one to its upper surface by very thin mud layers (mm-
27 scale) or mud drapes. The intermediate interval (b) is composed of symmetrical wave ripples passing
28 to megaripple cross bedding. The upper interval (c) is characterized by micro-hummocky cross stratification
29 expressed by successive lamina sets separated by low angle truncations surface and composed of parallel low-

1 angle curved lamina which dome upward (hummocks) passing laterally into laminae that are
2 concave upward (swaley).

3 Facies F22 (Fig. 5F and Fig. 6), is identified in the Si Moussa Formation of Middle Miocene age (Fig. 3). It
4 consists of alternating metric sandy bar and decimetric to metric highly bioturbated muddy layer. The bar is
5 composed of amalgamated lenticular metric cross stratified and cross laminated coarse-sandy micrite beds
6 displaying sharp basal surfaces, low angle cross-stratified (less than 10°) laminations and sets of sigmoidal cross
7 laminations delimited by reactivation surfaces. The beds are disturbed by convolute bedding, slumps, and ball
8 and pillow and may show decimetric desiccation cracks at their top.

9

10 Provenances and depositional environments reconstruction

11

12 Petrofacies interpretation

13 The five petrofacies identified (Fig. 2, photos A, B, C and D) according to Mount (1985) classification:
14 silty micrites, micritic siltstones, micritic sandstones, sandy micrites, and allochemic sandstones, are very similar
15 to those observed within the Eocene to Miocene sedimentary series outcropping in the North Western Rif
16 (Hamoumi 1995b; Hamoumi et al. 1995; Ouldchalha et al. 1995; Salhi et al. 1995). Their compositional mixing
17 indicate contemporaneous accumulation and sediment supply from both intra-basinal and extra-basinal sources
18 under the control of allocyclic (e.g. sea level, tectonics, climate) and/or autocyclic (depositional processes)
19 factors. The presence in the siliciclastic fraction of undulatory monocrystalline quartz with sometimes secondary
20 quartz overgrowths, polycrystalline quartz grains, volcanic and metamorphic rock fragments and micas
21 (muscovite, biotite and chlorite) and the roundness of heavy minerals suggest a provenance from sedimentary,
22 volcanic and high rank metamorphic sources. The existence of calcite lithoclasts which may include benthic and
23 planktonic foraminifera including e.g., *Orbitolina* and sometimes micritized *Calpionella*, indicate extrabasinal
24 carbonate sources including a source of Cretaceous age. The poor sediment sorting, as well as the presence of
25 rock fragments, feldspar and biotite is in favor of rapid erosion from a young and high relief continental source
26 and a short transport and rapid deposition. Alteration affecting feldspar and micas as well as small size and lower
27 frequency of feldspar suggest a hydrolyzing (humid to semi-humid) climate. The intra-basinal source provides
28 the shell fragments which results from reworking of in situ exoskeletons and glauconitic peloids. Algae and
29 rhombohedral crystals of dolomite, suggest nearshore to shallow marine depositional setting. Glauconite is

1 authigenic and forms in shallow marine environment under reducing to slightly oxidizing conditions (Pettijhon et
2 al. 1973, Odin 1985). The micritization which affects Calpionella is probably is inherited from the source. It can
3 neither be generated by organisms such bacteria or algae, nor be linked to burial compaction, because it does not
4 affect all microfossils.

5

6 Sedimentary structures interpretation

7 The sedimentary structures which characterize the sedimentary facies identified in the Mrayt Group series
8 revealed significant informations on the depositional and the post-depositional processes that control the
9 sedimentation. The primary sedimentary structures observed indicate erosion and deposition under the interplay
10 of waves, storms, tidal and fluvial currents.

11 The waves action is expressed by: symmetrical ripples (F1, F2, F10 and F21) and asymmetrical ripples (F1,
12 F2, F3, F6, F10, F12, and F15) which present characteristics of wave-ripple bedding (De Raaf et al. 1977), such
13 as: lateral variation in size and shape of the ripples in the same layer, offshooting and draping laminations
14 expressed by foreset laminae which ascend and overlap the flank of the adjoining ripple, composite internal
15 structure made up of an assemblage of differently structured, generally bidirectional lenses or multidirectional
16 lenses, parallel undulated lamination, pinching and swelling laterally and passing to incipient lenses, small lenses
17 of mud preserved in the trough of the ripple, swollen lens-like sets, undulating parallel laminations passing into
18 cross laminations, ripple cross laminated layers which display unidirectional cross lamina concordant with the
19 stoss side and irregular undulating lowerbounding surface. Waves action is also expressed by low angle cross
20 stratification (less than 10°) in coarse sandy micrite (F18 and F22), which results from parallel seaward-dipping
21 lamination in foreshore-backshore (Shahin et al. 2009).

22 Storm action is indicated by: hummocky cross stratification (F13), micro-hummocky cross stratification
23 (F20, and F21) and quasi planar laminated tabular sets (F19). The Hummocky cross stratification (HCS) was
24 introduced and described by Harms et al. (1975), it's produced by unidirectional and oscillatory flow generated
25 by storm events beneath the fair-weather wave base and above the storm weather wave base. It's widely
26 recognized both in modern environments in the shoreface (Howard & Reineck 1981) and in the upper offshore
27 (Swift et al. 1983). Micro-hummocky cross stratification occurs in open-coast intertidal flat, the HCS become
28 smaller in a landward direction because of a decrease of wave size (Yang et al. 2006). Quasi planar laminated
29 tabular sets are considered as proximal tempestites deposited from storm wave-generated oscillatory flows or
30 oscillatory-dominated combined flows (Jelby et al. 2019).

1 Evidence of tidal current action is expressed by the existence of typical facies and structures as layers of
2 sediments, periodically deposited in relation to daily and monthly tidal cycles and signature of reversing currents
3 (Boersma 1969; Dalrymple et al. 1978; Visser 1980; Terwindt 1981; Allen and Homewood 1984; Mowbray and
4 Visser 1984; Kreisa and Muiola 1986; Dalrymple and Makino 1989; De Boer et al. 1989; Tessier et al. 1989; Nio
5 and Yang 1989; Dalrymple, 1992). Tidal bundle or mud couplet (F1, F11, F15, F16, and F21) indicates changes in
6 current velocity and flow reversals related to daily tidal cycles. Sand laminae reflect alternating ebb and flood
7 episodes known as diurnal inequality, coarser laminae are deposited by dominant tide current (thick lamination)
8 and subordinated tide current (thin lamination) and mud drapes are formed during slackwater stages by
9 deposition of suspended mud. Alternation of thick and thin tangential laminae (F4, F9, F16) or sigmoid laminae
10 (F7, F11, F15, F16, F22) limited each one to its upper surface by very thin mud layer (F3, F8, F12, F20)
11 correspond to a tidal bundle related to daily tidal cycles. Sigmoid-shaped sets separated by reactivation surface or
12 mud drapes and made up of successive mud couplets (F8) result of tidal lateral accretion of a large-scale
13 bedform such as megaripples or sand waves during a dominant tide. Stacked sets of thin laminae which thicken
14 progressively from the bottom to the top and sets of thick laminae which thin progressively from the bottom to
15 the top (F1, F6, F7, F10, F11, F12, F15, F16, F21) are considered as a tidal rhythmites. These microsequences,
16 represent a vertical record of neap/spring tidal cycles fluctuations that occur during a lunar cycle. During spring
17 tidal excursion is at maximum and during neap tide, tidal excursion is at minimum. Successive intervals
18 exhibiting sigmoidal or tangential cross laminated cm-bundles, dipping in opposite directions (F11, F12) are
19 generated by the reversing currents which can be developed in tidal environment. The cross laminated beds
20 deposited during ebb tide dip in opposite direction of those formed during flood tide. Reactivation surface (F1,
21 F7, F15, F19, and F22) is a minor erosion surface between cross-strata which results from partial erosion by
22 reversing current during an asymmetrical tidal cycle. The lower bedform is eroded back by the reverse current
23 and buried by a new advancing bedform.

24 Interbedded layers of fine sandstone and mudstone expressed by: 1) ripples with small lenses of mud
25 preserved in the trough (F1, F2, F15), 2) Interbedded rippled sandy layers and continuous mud drapes
26 overlapping the ripple troughs and crests (F1, F2) and 3) well preserved micritic siltstone or sandstone lenses,
27 embedded within muddy layer (F2) are respectively flaser bedding, wavy bedding and lenticular bedding. These
28 sedimentary structures are characteristics of tidal deposits in intertidal zone and are related to tidal cycles, mud
29 deposition is favored by the existence of slack tides (Reineck and Singh 1980; Dalrymple and Makino 1989). In
30 the flaser bedding facies, ripple beds are deposited during periods of current activity and mud lenses result from

1 mud in suspension when energy of currents decreases. Wavy beddings develop when preservation of mud is
2 possible and lenticular bedding reflects more favorable conditions for deposition and preservation of mud than
3 sand. Linguoid ripples (F5) and straight-crested ripples (F3 and F6) are generated in tidal flat by unidirectional
4 current (Reineck and Singh 1980). Mud drapes (F1, F4, F6, F7, F10, F11, F12, F16, F19 and F21) may be found
5 in various environments, their occurrence with typical tidal structures and facies is in favor of tidal origin. They
6 result from deposition of concentrated suspended mud during the slack-water stage

7 Sedimentary structures related to fluvial currents are: asymmetric ripples characterized by a planar base and
8 planar cross-lamination (F2, F5 and F8), flute casts (F10, F11, F12, F15, F16) and tool casts: groove casts (F9,
9 F10, F11, F12), bounce cast (F9) and prod casts (F9, F10, F11). Flute casts is the molding of a flute mark, which
10 is a tongue-shaped scour produced into mud by a turbulent flow of water. Tool casts are molding of tool marks
11 which are produced by larger particles (e.g., pebbles and shell) on soft sediments under action of turbulent flow.
12 Groove marks are caused when fragments are dragged along, prod casts and bounce casts are produced when
13 fragments bounced along or hit the substrate. Flute casts and tool casts are commonly linked to turbidity currents
14 in deep marine settings. However they can form also in the fluvial-to-marine transition zone under action of
15 transitional flows whose turbulence results from the density differences between sediment-laden fresh and
16 marine water. Fluvial current action is also demonstrated by the texture and the characteristics of the three
17 conglomerate levels (Facies F17) such as the AB-plane type imbrications.

18 Post depositional and secondary sedimentary structures (Fig. 8) include desiccation cracks, water escape
19 structures, load structures, soft sediment deformations and biogenic structures. Desiccation cracks (F1, F2, F3,
20 F4, F5, F7, F9, F11, F13, and F22) are subaerial sedimentary structures which form when wet sediments dries up
21 and contracts under evaporation processes. They occur in settings submitted to subaerial exposures: fluvial
22 levees, shore of lakes, delta plain and tidal flat. Dish and pillar structures (F15 and F19) are water escape
23 structures that form in unconsolidated sediments during stages of rapid deposition in deep sea fan and/or deltaic
24 and fluvial systems (Lowe 1975).

25 Load casts (F18, F19, F20, F21) and flame structures (F10), form in response to deposition of layer of
26 denser sediments (sand) over on a less-dense hydroplastic layer (mud), especially during high sedimentation rate.
27 The overloading lead to the sinking of the sand layer in the form of highly irregular protuberances and lobes (load
28 casts) or projecting curved, pointed tongues of mud as wavy or "flame" shaped into the overlying sand (flame
29 structures). Convolute beddings (F8, F10, F11, F12, F15, F16, F18, F19, and F22) are centimetric crumpling and
30 folding of parallel laminae or foreset laminae of ripple bedding. They occur in fine grained soft-sediment in

1 various settings from deep- marine to nearshore and fluvial environments, and they occur frequently are in deltas
2 and intertidal flats. They can be produced in more than one way (Reineck and Singh 1980 and reference therein):
3 liquefaction, shearing action of currents, down-slope movement favored by the existence of a slope, high
4 sedimentation rate, and seismic shaking.

5 Slump structures (Fig.8) observed in Sandstone-pelitic Formation and Si Moussa Formation, consist of a
6 metric size, complex fold patterns often overturned. They result from movement and displacement of
7 unconsolidated sediments induced by high sedimentation rate, sliding down a slope, faulting and seismic shaking.
8 Balls and pillows (F18, F22), may occur as rounded masses of coarse sediments (pseudonodules) in fine grained
9 matrix or as isolated pillows with curved and deformed internal laminations in a sandstone layer. They result in
10 unconsolidated sediment under a physical shock which causes instability and rupturing of the sediment layer,
11 generally in relation with tectonics.

12 The trace fossils (Fig.9) observed includes *Ophiomorpha* burrows (F10, F15, F16, and F18) Skolithos
13 burrows (F15), *Cruziana* (F8 and F9), *Psilonichus* Y-shaped burrows (F3), *Zoophycos* (F16) and *Paleodyction*
14 tunnels (F8 and F9). *Ophiomorpha* is considered as a part of the Skolithos ichnofacies (Seilacher 1967) and is
15 produced by crustaceans such as shrimps (Frey et al. 1978) in nearshore and shallow marine depositional
16 environments (Boggs 1995; Buatois and Mángano 2011), Skolithos belong to Skolithos ichnofacies
17 (Seilacher 1967) is produced by a variety of organisms and commonly associated with lower intertidal to shallow
18 subtidal settings in moderate to high-energy conditions. *Cruziana* burrow belong to *Cruziana* ichnofacies is
19 considered typical of subtidal above storm wave base, but was recognized in intertidal zone (Pandey et al 2014).
20 *Psilonichus* may be produced by: decapod crustacean, shrimp or crab, it occurs in estuary to backshore
21 sedimentary settings (Nesbitt and Campbell 2006). *Zoophycos* is considered as feeding or moving trace, it was
22 associated for a long time with deep marine sediments, often turbidites. However it has been reported from
23 shallow marine storm deposits (Zhang and Zhao 2016; Belghouthi et al. 2020) and nearshore settings
24 (Knaust 2004). *Paleodyction* burrows consist of a regular hexagonal or polygonal network of tubular tunnels. They
25 are commonly linked to deep -water Nereites ichnofacies (Seilacher 1967) and were identified in many flysch
26 successions and at present day abyssal environments. However they has been documented in prodelta
27 environments, in relatively shallow epicontinental basin, and in mid -to -deep -shelf environments of Upper
28 Triassic and Middle Jurassic in Iran (Fürsich et al. 2007), and in association of trace fossils belonging to *Cruziana*
29 ichnofacies in the Devonian of Pennsylvania (Metz 2012). Y-Shaped burrows (*Psilochinus*) indicate a shallow
30 marine coast (Frey et al. 1978).

1

2 Sedimentary facies associations and sequences interpretation

3 The facies identified are grouped into three facies associations: Tide dominated estuary facies association, tide
4 dominated delta facies association, and open-coast tidal flat facies association. (Fig.11).The estuary facies
5 association is composed of a tidal flat sub-association (F1 F2, F3, F4,) and an estuary channel sub-association
6 (F5, F6,F7). In the tidal flat sub-association, FaciesF1 exhibits mud couplets, wavy bedding, flaser bedding, mud
7 drapes and wave ripples. These sedimentary structures indicate deposition from tidal current and waves. Mud
8 couplet reflects daily tidal cycles and mud drapes result from deposition of concentrated suspended mud during
9 the slack-water stage. Occurrence of wavy bedding and flaser bedding is frequent in tidal setting where the slack
10 tides favors mud deposition (Reineck and Singh 1980; Dalrymple and Makino 1989).

11 Facies F2 shows a vertical evolution from flaser bedding to lenticular bedding through wavy bedding which
12 is considered as diagnostic of strongly tide influenced intertidal flats. Facies F3 comprises a slightly deformed
13 interval and asymmetric ripples related to wave and tidal currents. Combined- flow and wave –induced structure
14 and bedding characterize exposed tidal flat setting. The slight deformations of the lower interval may suggest a
15 high sedimentation rate. Facies F4 represents deposition in a tidal creek or gullie illustrated by erosively
16 undulating base and tidal current induced structures such as: sets of parallel plane laminae, tangential cross
17 laminated cm-bundles, reactivation surfaces and mud drapes. Successive tangential bundles and reactivation
18 surfaces are related to diurnal inequality of tides.

19 In the estuary channel sub-association, Facies F5 consists of an erosional based succession displaying a
20 basal lag rich in mud pebbles, passing to silty micrite interval with unidirectional flow ripples which in turn is
21 overlain by an interval with wave ripples. The top shows linguoid ripples and centimetric to decimetric
22 desiccation cracks. This facies results from deposition within a distributary channel under the interplay of tide
23 currents and waves. Mud pebbles form at least in two stages: 1) a breakage of muddy bed by desiccation during a
24 dry periods, bioturbation or erosion by currents which results in the formation of muddy chunks and flakes, and
25 2) reworking of the intraformational clasts by storms or tidal currents and accumulation on the erosional surface
26 as lag deposits. Linguoid ripples occur in tidal flat under unidirectional current (Reineck and Singh 1980).

27 Facies F6 comprises neap/spring tidal rhythmites mud drapes, wave ripples and desiccation cracks at its top.
28 This facies is interpreted as a tidal pointbar deposit under the interplay of tide currents and waves. Tidal point
29 bar forms within active distributaries of the estuary and extends from shallow to supratidal settings, thus
30 desiccation cracks occur during subaerial exposure stage.

1 Facies F7 displays neap spring tidal rhythmites, sigmoid-shaped sets made up of successive
2 mud couplets, mud drapes, reactivation surface and desiccation cracks. It is interpreted as distributary channel
3 fill, where tidal action is expressed by the most diagnostic structures of tidal origin: neap /spring tidal rhythmites,
4 sigmoidal bundles, mud drapes and reactivation surface. The desiccation cracks result from subaerial
5 exposure related to shallowing due to sedimentation and channel abandonment. Combined-flow and wave-
6 induced structures and beddings suggest sedimentation in a tide dominated and wave influenced mixed tidal
7 flat. The presence of desiccation cracks indicating repeated emergence. The existence of distributary and tidal
8 channel fill is also supported by the existence of marine and littoral organisms such as benthic and planktonic
9 foraminifera, Calpionella and bioclasts of: gastropods, bivalves, echinoderms, bryozoans and algae. Tide
10 dominated estuary receive sediments both from the river at the head of the estuary and from adjacent shelf by
11 tidal currents.

12 The delta facies association includes a lower delta plain sub-association (F3, F4) a tide dominated delta
13 front platform sub-association (F9, F10, F11 F12, F13 F14, F15, F16, and F17), and a prodelta (F8). In the delta
14 plain sub-association, facies F3 suggests deposition in tidal flat under combined- flow and wave action and
15 facies F4 represents tidal creek fill. In the front delta platform sub-association, Facies F9 display an erosional base
16 with tool casts (grooves casts, prod casts and bounce casts), Paleoduction tunnels, tangential cross
17 laminations and desiccation cracks at its upper bounding surface. This facies result from transitional flows in the
18 front delta slope. Tangential cross laminations are induced by unidirectional flow. Tool casts can form in such
19 fluvial-to-marine transition zone where the interaction of sediment-laden freshwater river flux and tidal currents
20 generates turbulent eddies and strong shears Paleoduction has been documented in deltaic environments, in
21 relatively shallow epicontinental basin. The desiccation cracks at the top of the bed are related to subaerial
22 exposure episode due to swallowing of the setting.

23 Facies F10 and F11 has an erosive base exhibiting prod casts (F10) and flute casts (F10, F11) induced
24 by transitional flows whose turbulence results from the interaction of fluvial and marine process. Gravity-driven
25 transport may occur when river are discharging peak sediment loads onto an energetic marine environment.
26 This mode of sediment transport has been highlighted in several delta studies. (e.g. Wright and Friedrichs 2006).
27 Their internal structure which can be affected by flame (F10) and convoluted beddings (F10, F11) is made up of
28 alternating wave ripples and tidal sedimentary structures such as: neap spring tidal rhythmites, wavy bedding,
29 sigmoidal cross laminations, opposite directions of fore set laminations in adjacent layers, reactivation surfaces.
30 The upper surface of these facies may show mud pebbles (F10, F11) and decimetric-scale desiccation cracks

1 (F11) and the base of F10 base exhibits Ophiomorpha burrows (F10). The presence of mud pebbles indicates an
2 accumulation at the top of beds during episodic storm events. F12 displays alternating wave ripples which may
3 be disturbed by convolute bedding and tidal structures: neap spring tidal rhythmites, tangential cross laminated
4 cm-bundles dipping in opposite directions in adjacent layers and mud drapes. This facies result from the
5 interplay between tidal currents and waves.

6 Facies F10, F11 and F12 are interpreted as tidal sand ridges deposits which developed in the delta front
7 platform. This part of the deltaic system is controlled by the interplay between river discharges and fluvial
8 sediment load and marine processes: tides, waves, and episodic storms. The vertical succession of sedimentary
9 structures indicate rapid transition from subtidal to intertidal setting, desiccation cracks are related to subaerial
10 exposure period due to swallowing of the setting. The presence of Ophiomorpha burrows is also indicative of a
11 high energy sublittoral or shoreface environments. This trace fossil occurs from littoral to shallow-marine
12 paleoenvironments (Buatois and Mangano 2011).

13 Facies F13 corresponds to a storm event deposit as indicated by its geometric characteristics: erosional
14 undulating base and erosive top exhibiting metric scale wavelength hummocks, and its internal structures
15 expressed by metric scale hummocky cross stratification. Decimetric desiccation cracks and soft pebbles at the
16 top indicate period of subaerial emergence.

17 Facies F14, F15, F16 and F17 represents channel fill deposits at the mouth area of front delta. Facies F14,
18 F15, F16 have in common a highly erosive base with flute casts and an interval corresponding to a lenticular
19 fining upward microconglomerate which may comprise tangential cross-stratification. In Facies F15 and F6, this
20 interval is surmounted by a fining upward sequence showing grading from allochemic sandstones which may
21 be affected by dish and pillar structures and convolute bedding (F15) into micritic siltstone or silty micrite. The
22 sequence in F15 exhibits waves rippled and tidal structures: mud couplets tidal rhythmites reactivation surfaces,
23 sigmoidal tidal bundle and flaser bedding as well as mud pebbles, and Ophiomorpha and Skolithos burrows at its
24 top. The sequence in F16 displays only tidal structures: neap spring tidal rhythmites, sigmoidal bundle, mud
25 drapes and reactivation surface and Zoophycos, Ophiomorpha and Skolithos burrows traces at its top.

26 Facies F14 is interpreted as being a channel fill deposit from unidirectional turbulent flow. Facies F15 and
27 F16 record different stages of channel initiation and fill, scouring, flute casts and normal grading of the lower
28 interval are related to unidirectional turbulent flow. The filling of the F15 channel was made first under action
29 tidal current and with shallowing upward due to sedimentation, the filling continued with waves. In the case of
30 F16 filling was made only by tidal currents. The existence of nearshore to marine organisms and shell fragments

1 in facies F14, F15, and F16 confirms the intrusion of marine and coastal currents in the channels. Ophiomorpha
2 and Skolithos burrows belong to skolithos ichnofacies (Seilacher 1967) which is diagnostic of nearshore and
3 shallow marine depositional environments. Zoophycos has been reported from shallow –marine storm deposits
4 (Zhang and Zhao 2016; Belghouthi et al. 2020) and nearshore settings (Knaust 2004). Dish and pillar structures
5 consist of fluid escape structures which results of quick packing due to high sedimentation rate. Convolute
6 bedding are common in front delta and prodelta settings, they may form during gravity-driven flows or tectonic
7 events.

8 Facies F17 is interpreted as fluvial deposits based on the dimension, the lithology, the composition, the
9 texture and the sedimentary structures that characterize fluvial facies (Miall 1992). The shape of the clasts
10 underlines a short transport distance. The absence of sedimentary structure and fabric as well as the poor sorting
11 of the massive polymictic, texturally immature matrix supported conglomerate (Subfacies F17a), suggest
12 deposition by gravity flow. Fine-grained sandstone bed (Subfacies F17b) might have resulted from deposition by
13 vertical accretion on the top of channels sand bars during low flow régime. Clasts-supported conglomerate unit
14 (Subfacies 17c) is interpreted as channel lag deposits, based on its highly erosive base, lenticular shape, and texture
15 especially the AB-plane type imbrications of the clasts. The coarse sandstones exhibiting planar and cross-
16 stratified beds separated by erosional surfaces may be attributed to vertical accretion during lower flow regime, or
17 to the migration of sand dunes and transverse bars in shallow water stream channel. These subfacies result from
18 fluvial discharges in response to flooding stages and reactivation of detrital inputs due to tectonic events and
19 uplift of the source area. Marine to nearshore bioclasts such as bivalve shells of the matrix of the clast supported
20 conglomerate and the coarse sandstone, confirm deposition at the mouth of delta submitted to flood tides.

21 Facies F8 consist of predominant muddy deposit with centimetric alternation of silty micrite displaying
22 planar parallel laminations or tabular cross-laminations that may be disturbed by convolute bedding, and intense
23 bioturbation. This facies can be formed in an offshore or in a prodelta this last hypothesis is the most probable
24 because of its association with deltaic facies at the base of upward coarsening sequence. Convolute bedding are
25 frequent in such setting and may be induced by gravity driven transport in the delta slope or under high rate of
26 sedimentation. Intense bioturbation indicates a low-energy setting with normal oxygenated conditions. The
27 presence of Paleoduction tunnels has been documented in prodelta environments (Fürsich et al. 2007).

28 In the open-coast tidal flat facies association, Facies F18 is interpreted as nearshore sand bar based on low-
29 angle cross laminated sets separated by erosional surfaces. Low-angle cross laminated result from mega ripples
30 migration and may be generated by waves processes during fair weather periods (Wright and Short 1984).

1 Occurrence of Ophiomorpha trace fossil is consistent with nearshore environments. Load casts may result from
2 high sedimentation rate. Convolute bedding, ball and pillow and slumps may be induced by tectonics.

3 Facies F19 is interpreted as proximal tempestite deposited from storm wave-generated oscillatory-dominant
4 combined flows (Jelby et al. 2019) and tidal currents, based on the existence of erosional limits, quasi planar
5 laminated tabular sets, reactivation surfaces and mud draps. Association of proximal tempestites and tidal
6 structures are in favor of a cyclic deposition by storm and tide currents in an open coast tidal flat. Water escape
7 structures and convolute bedding which may affect this facies, might have been induced by a high sedimentation
8 rate or storm waves. Soft-sediment deformation structures are well documented in tempestites and interpreted as
9 the result of liquefaction triggered by the stress induced by storm waves (Jelby et al., 2019 and references
10 therein).

11 Facies F20 is considered as storm deposit in intertidal flat based on the existence of erosional bounding
12 surfaces, planar parallel lamina and micro-hummocky cross stratification. Micro-hummocky cross stratification
13 occurs in open-coast intertidal flat, the HCS become smaller in a landward direction because of a decrease of
14 wave size (Yang et al. 2006). Load casts express a high sedimentation rate.

15 Facies F21 consist of coarse-sandy micrite bed displaying mud couplet, wave ripples passing to mega-ripple
16 cross bedding and micro-hummocky cross stratification. This facies is generated in the intertidal zone under the
17 tide, waves and storm action.

18 Facies F22 corresponds to a nearshore sand bar generated by fair weather wave and ebb or flood delta
19 which developed in tidal inlet by tidal current. Wave signature is expressed by the existence of low angle cross-
20 stratified (less than 10°) laminations. Influence of tidal currents is recorded by the sets of sigmoidal cross
21 laminations delimited by reactivation surfaces. Occurrence of decimetric desiccation cracks at the top of beds
22 suggests sedimentation in nearshore setting submitted to subaerial exposure. Convolute bedding, ball and pillow
23 and slumps are probably induced by tectonics.

24 Open-coast tidal flat recorded by Facies association (F18, F19, F20, F21, and F22) developed under action
25 of tides, fair weather waves and storm action. It corresponds to a sandy open coast tidal flat in the classification of
26 Daidu (2012) which is characterized by: 1) abundance of storm-generated structures, 2) scarcity of tidal-channel
27 deposits and 3) abundance of structures created by combined flows or the interactions of waves and tides.
28 According to this author, such depositional environment is common in the open-mouth estuaries of small river
29 and the adjacent strand plain.

30

1 Discussion

2

3 The Mrayt Group deposits have been previously described as siliciclastic sediments: quartzarenite and
4 sublitharenites (Tejera de Leon 1993) the petrographic analysis of thin sections performed in this study, has
5 shown that the sediments are not siliciclastic deposits but rather mixed siliciclastic/carbonate components. The
6 petrofacies recognized according to Mount classification (1985) are: silty micrite, micritic siltstones, micritic
7 sandstones, sandy micrite, and allochemic sandstones. They are very similar to those observed within the Eocene
8 to Miocene sedimentary series outcropping in the North Western Rif (Hamoumi 1995b; Hamoumi et al. 1995;
9 Ouldchalha et al. 1995; Salhi et al. 1995). Furthermore, such mixed deposits are quite common in ancient and
10 modern depositional environments (see references in Chiarella et al. 2017). These new findings are even more
11 important than mixed siliciclastic / carbonate rocks in the Rif belt are not well encoded. The tendency has been to
12 ignore the mixed composition and to consider them as pure siliciclastic which results in wrong
13 nomenclatures. Precise petrographic analysis and classification are necessary for accurate naming and classifying
14 sedimentary rock which is in turn essential to reconstitute provenance (nature and composition of the sediment
15 source, relief and climate in the source areas), as well transport and sedimentation processes, and diagenetic
16 history. They are also fundamental tools in hydrocarbon exploration and engineering, according to Chiarella et
17 al., (2017), a correct identification of different types of mixing and the scale of their occurrence is essential for
18 petrophysical properties (porosity, permeability) identification and reservoir models reconstruction in
19 hydrocarbon exploration and exploitation.

20 The compositional mixing indicates contemporaneous accumulation and sediment supply from both intra-basinal
21 and extra-basinal sources. The intra-basinal components: shell fragments, algae glauconitic peloids rhombohedral
22 crystals of dolomite and mudclasts, suggest nearshore to shallow marine depositional settings submitted to flood
23 tides. The extra-basinal source that provides the siliciclastic components and detrital carbonates, may
24 correspond to the geological sections outcropping along the African margin which consists of Paleozoic
25 basement of detrital dominance, folded, metamorphosed and granitized during Hercynian orogeny and its cover,
26 the Meso-Cenozoic terranes, which are essentially carbonates. The presence of Cretaceous benthic foraminifera
27 of the genus *Orbitolina* and other micritized foraminiferal test argues their provenance from the Meso-Cenozoic
28 sediments. This hypothesis is supported by the results of palaeocurrents analysis carried out in this work that
29 indicate a transport path from SSE to NNW, and those of previous works (Cazzola and Critellis 1987; Morley
30 1992; Tejera de Leon 1993).

1 Previous works have proposed deposition of the Mrayt Group successions in marine (distal shelf and
2 continental slope) of foredeep basin. They interpreted as a sedimentary prism adjacent to the outer edge of a
3 storm dominated platform, which passes to deep sea fan system (Raissouni et al. 2008), or as synorogenic
4 turbidites referred to deep sea fan and reworked and redeposited slope flows in an abyssal plain (Morley 1992;
5 Tejera de Leon 1993). Sedimentary facies reconstruction and interpretation performed in this work indicates that
6 deposition of Mrayt Group sediments was realized in littoral and shallow marine environments: tide dominated
7 estuary, tide dominated delta and open-coast tidal flat.

8 In these depositional environments, sedimentation took place under complex hydrodynamics strongly
9 influenced by river discharge, tidal currents, waves and storms action. Evidence of tidal current is expressed by
10 unique sedimentary structures and facies that can only be produced by tides such as: layers of sediments,
11 periodically deposited in relation to daily and monthly tidal cycles and signature of reversing currents (Boersma
12 1969; Dalrymple et al. 1978; Visser 1980; Terwindt 1981; Allen and Homewood 1984; Mowbray and
13 Visser 1984; Kreisa and Moiola 1986; Dalrymple and Makino 1989; De Boer et al. 1989; Tessier et al. 1989; Nio
14 and Yang 1989; Dalrymple 1992). The waves action is indicated by typical wave-generated symmetric and
15 asymmetrical ripples (De Raaf et al. 1977) and low angle cross stratification (Shahin et al. 2009). The storm
16 signature is expressed by hummocky cross stratification (Harms et al. 1975), micro-hummocky cross
17 stratification, (Yang et al. 2006) and quasi planar laminated tabular sets (Jelby et al. 2019). The fluvial action is
18 recorded by current asymmetric ripples, flute casts and tool casts (groove casts, bounce casts and prod casts) and
19 the the AB-plane type imbrications of the pebbles of the conglomerates. Nearshore environments are also
20 suggested by: i) the presence of Skolithos and Ophiomorpha burrows considered part of the Skolithos ichnofacies
21 (Seilacher 1967), ii) Psilochinus Y-shaped burrows which indicate a shallow marine coast (Frey and
22 Pemberton 1978), iii) desiccation cracks indicating repeated emergence and iv) the presence of shell debris and
23 abundant mud clasts in the floor the channels.

24 Sedimentation occurred in “the Maghreb basin” defined by Bouillin (1986), extending between the
25 North African margin and the Internal zones domain during the Mesozoic-Paleogene interval (Wildy 1983),
26 under the interplay of tectonics and subsidence, eustasy, climate and sediment supplies. Evolution of the tectonic
27 regime was guided by the complex subduction events and associated collisions between the African and Eurasian
28 continental plates during the late Mesozoic and Cenozoic (Dewey et al. 1989; Srivastava et al. 1990; Leprêtre et
29 al. 2018 and references therein). After the Early Eocene Climatic Optimum (EECO), the evolution of the
30 Cenozoic climate recorded gradual trends of warming and cooling (Zachos et al. 2001). Following the Ypresian

1 high sea level, Cenozoic period was marked by short-term sea level fluctuations due to the increasing influence
2 of glaciation. (Haq et al.1987).

3 Three depositional system intervals are recognized in the Mrayt Group successions from Early Eocene to Mid
4 Miocene: tide dominated estuary, tide dominated delta and open-coast tidal flat. The first interval extended from
5 Early to MiddleEocene, it records a tide dominated estuary system composed of a tidal flat and estuary channels.
6 The tidal flat is characterized by tidal rhythmites and fining upward heterolithic successions showing regular
7 changes vertically from flaser bedding through wavy bedding and lenticular bedding, (F1 and F2), surmounted
8 by tidal creek or gully (F3 and F4). The estuary channel sub-association comprises, distributary channel fill
9 (F5 and F7), tidal point bar (F6).

10

11 The Mrayt Group Eocene estuary system is a coastal plain estuary type where tidal action is expressed by
12 the most diagnostic structures of tidal origin. Tide dominated estuaries are those in which tidal currents play
13 dominant role at the mouth(Dalrymple et al.2012). They form generally in shelves that are large enough to
14 amplify the oceanic tidal wave. Initiation and development of estuarine system depends on three principal
15 factors: rise in sea level, climate and subsidence. According to Dalrymple et al.(1992) an estuary is a
16 transgressive coastal environment at the mouth of a river, that receives sediment from both fluvial and marine
17 sources and that contains facies influenced by tide, wave and fluvial processes. The climate controls the amount
18 of precipitation and therefore the fluvial flow regime as well as the nature and quantity of the sediment supplies.
19 Recent estuaries occur in temperate and tropical regions which are characterized by frequent and abundant rains
20 and the existence of large rivers. Subsidence is necessary for the preservation of tidal deposit in as much as a part
21 of the sediments deposited by a tidal current if not all may be eroded by the opposite tidal current.

22 The Mrayt Group estuary system was initiated by the drowning of an existing river valley during the Early
23 Eocene (Ypresian) sea level raise (Haq et al.1987). Development of this estuarine system was favored by the
24 subsidence and a warm and humid climate. After the end of the Paleocen-Eocene Thermal Maximum (PETM) at
25 56 million years ago, the Eocene climate began with a warming(Zachos et al. 2001).According to Brinkhuis et al.
26 (2006) the warm greenhouse conditions of the Early Paleogene period (55-45 Myr ago) probably increased
27 precipitation. Moreover, the climate in the Sahara during the Eocene would have been humid and warm
28 (Swezey2009).

29 The Mid-Upper Eocene gap in the Mrayt Group succession could be explained by erosion or by an
30 interruption in deposition. This last hypothesis seems the most plausible. Non deposition may be attributed to the

1 combination of the effects of lowering in eustatic sea level and tectonic uplift. Major sea level falls occurred at the
2 latest Ypresian and the latest Bartonian (Haq et al. 1987). Moreover, the Middle Late Eocene kinematic
3 reorganization related to the strong coupling between the Eurasian, Iberian and African plates resulted in the
4 development of intracontinental belts and compressive deformation at the scale of the west Mediterranean region
5 (Leprêtre et al. 2018 and reference therein).

6 The second interval records the development of a tide dominated deltas during Early Oligocene to Early
7 Miocene period. Recognition of these depositional systems is based on the existence of three genetically linked
8 facies and facies association in the same succession: lower delta plain facies association, delta front platform
9 facies association and prodelta facies. The lower delta plain sub-association includes tidal flat (F3) and (tidal
10 creek or gully (F4). The tide dominated delta front platform sub-association includes: deposit of transitional
11 flows in the front delta slope (Facies F9), tidal sand ridges (Facies F10, F11 and F12), channel fill deposits at the
12 mouth area of front delta (Facies F14, F15, F16 and F17) and a prodelta facies (F8).

13 Recognition of tide dominated delta is also based on the typical criteria commonly admitted for delta
14 identification and the type of delta discrimination. 1) Coexistence of sedimentary structures and facies indicating
15 a combination of the effects of river discharge, wave, storm and tidal processes 2) Thick predominately clastic
16 successions which pass from subaqueous (offshore and shoreface) facies upwards into subaerial (intertidal flat
17 and fluvial channel). 3) Typical coarsening upwards sequence from prodelta to distributary channel and sand
18 bars interfingering with interdistributary muds. 4) Repeated progradation within a depocenter. 5) Occurrence of
19 the coarsest sediments in the boundary zone between the delta -front platform and slope and in the prograding,
20 distributary -mouth channel bars.

21 Tide dominated delta are those where tide currents are the dominant process controlling sediment dispersal
22 (Galloway 1975). The criteria which serve to distinguish tide dominated delta from the other deltaic systems are:
23 the existence of typical tidal sedimentary structures, sedimentary facies and sequences in the mid to upper part of
24 the delta front, the distributary tidal mouth bar and the lower delta plain successions. These tidal indicators
25 are: mud couplets, neap spring cycle, tidal rhythmites, bidirectional structures, reactivation surfaces, upward
26 fining succession, regular changes vertically from flaser bedding through wavy bedding and lenticular bedding,
27 tidal creek fill, distributary channel fills, tidal sand ridges. The criterion which serves to distinguish tide
28 dominated delta from other tidally influenced settings is the "S" shaped sedimentary succession that tends to be
29 heterolytic and both coarsening and fining upward (Goodbread and Saito, 2012). Additional criteria in favor
30 of deltaic interpretation are: 1) decimetric desiccation cracks and soft pebbles which indicate period of subaerial

1 emergence, 2) convolutes bedding which may be induced by gravity driven transport in the delta slope or under
2 high rate of sedimentation. 3) Intense bioturbation which indicates a low-energy setting with normal oxygenated
3 conditions, 4) mixing of marine to brackish fauna with detrital sediments from hinterland due to saltwater
4 transport by flood tides.

5 The direction of flow in this delta has been reconstructed based on by the paleocurrent measurements of 48
6 flute casts identified in all the studied outcrops. The paleocurrent flow as revealed by the rose diagram indicates
7 a transport path from SSE to NNW (Fig. 10) and is consistent with that proposed by the previous works (Cazzola
8 and Critelli 1987; Morley 1992; Tejera de Leon 1993). Other deltaic systems have been recognized in sections of
9 the same age in the North Western Rif (Hamoumi et al. 1995; Oueldchelha et al. 1995), which was considered by
10 previous works as deep sea fan deposits.

11 The initiation and the development of the Mrayt Group deltas were favored by the combination of major
12 factors: tectonics and subsidence, sea level fluctuations, climate and sediments supplies. Delta construction was
13 favored by the creation of depocenters induced by tectonics and subsidence. An Oligocene to Early Miocene
14 extensional phase representing one of the two periods of strong mechanical coupling between Africa and
15 Europe/Iberia plates, is recorded (Leprêtre et al. 2018 and references therein). Evidence for the tectonic control
16 during sedimentation is revealed by synsedimentary faults and soft sediment deformations (slumps, ball and
17 pillow). Tectonic activity and uplift in the drainage basin is attested by large amount of detrital sediment supplies
18 induced by rejuvenation of the source areas following the end Eocene tectonic uplift in relation to the major pre-
19 oligocene compressional event (Leprêtre et al. 2018 et references therein). It's also confirmed by the presence of
20 sedimentary structures induced by rapid deposition and increase in sedimentation rates (water escape structures,
21 load structures). Most present day tide dominated delta is situated in tectonically active regions (Goodbread and
22 Saito 2012).

23 Delta formation was also favored by the relatively higher sea level recorded at the Early Rupelian (Haq et
24 al. 1987). Delta confined to the shelf in shallow water is deposited during times of relatively high sea level. In
25 addition, tide dominated delta are more generally highstand features as adequate tidal energy is less well
26 developed during lowstand (Goodbread and Saito 2012). The climate plays a major role in both the catchment-
27 based forcing of sediment production and fluvial transport. Tropical climatic conditions in the Eocene has
28 changed from warm subtropical in the Eocene. The gradual cooling which occurred during the Eocene - Oligocene
29 transition at 34 million years ago (Zachos et al. 2001), should be associated with humidity and precipitation as
30 indicated by: i) the importance and quantity of detrital supplies and ii) alteration affecting feldspar and micas as

1 well as small size and lower frequency of feldspar. Moreover, it appears that during Oligocene,north-flowing
2 fluvial systems became a predominant feature across some parts of northern Africa during this time.
3 (Swezey2009)and North Africa was closer to the equator (Guiraud et al.2005).

4
5 Described facies and facies association occur in three progradational vertically stacked stratigraphic units.
6 Each unit shows an upwards coarsening succession from theprodelta mudstones,gradationally overlain by delta
7 front tidal bars, followed by erosively basedistributarychannels.The uppermost unit is overlain by lower delta
8 plain deposits. Development and evolution of these stratigraphic units were realized by repeated progradation
9 and abandonment within a depocenter dictated by fluctuations in sediment supply, subsidence and sea-level. In
10 the first two units, deltaic deposition occurs during the Rupelian relatively high sea-level (Haq et al.1987). The
11 higher stratigraphic unit is composed of three sub units, the lowers one is an upwards coarsening
12 successionsimilar to the first units with prodelta deposits gradationally overlain by delta front channel fill and
13 tidal bars. The second subunits is composed of stacked metric erosively basedistributary channels and the third
14 subunit is a lower delta plain succession.

15 Progradation of the first subunit was favored by tectonic and climate,the major sea level fall which
16 occurred near the Rupelian-Chatian boundary (Haq et al 1987), was compensated by compressive tectonics. A
17 significant compressional event was recorded in the tell Rif system during pre-Late Oligocene (Leprêtre et al.,
18 2018 and references therein).In addition, the tectonics allowed the source reactivation. Deposition of the second
19 subunit of the mouth areas is related to the development of an extensive fluvial systems which was favored by:i)
20 the persistence of decline in sea level, forced regression of the shoreline drives delta progradation and potentially
21 downward incision, ii)continued tectonic uplift of the hinterland and iii) enough rainfall, north-flowing fluvial
22 systems was a predominant feature northern Africa in during the Oligocene (Swezey 2009). The third subunit
23 correspond to the lower delta plain reflect deposition during rising relative sea level and creation of
24 accommodation space behind the delta front.This transgression would have been coincident with the higher
25 eustatic sea level (Haq et al.1987) and generally warm climate that characterized the late Middle Miocene
26 (Zachos et al.2001).

27 The third interval is a sandy open-coast tidal flat during Early Mid Miocene. Recognition of this
28 depositional system is based on the existence ofrhythmic alternation of nearshore sand bars generated by fair
29 weather waves (facies F18 and F22), storms (facies F20) storms and tidal currents (facies F19) and wave and
30 tidal current (facies F21). Nearshore environment is also indicated by centimetric to decimetric desiccation

1 cracks and Ophiomorpha burrows. Sandy open-coast tidal flats are common in the open-mouth estuaries of small
2 river and the adjacent strand plain (Daidu 2012). This stratigraphic unit expresses the abandonment of the deltaic
3 sedimentation and the installation of a wave storms and tide dominated open tidal flat. It coincides with
4 relatively high sea levels recorded during Aquitanian, Burdigalian, Langhian and Lower Serravallian (Haq et
5 al. 1987).

6 Sedimentation was favored by enough rainfall to support the development of extensive fluvial systems in
7 the hinterland. The global cooling induced by the establishment of the major ice-sheet on Antarctica (Frakes et al.
8 1992) was interrupted by warm intervals. A warming trend was recorded from the Lower Miocene to the Mid
9 Miocene where the warm phase peaked in the climatic optimum (Zachos et al. 2001). Sediment supplies have
10 been ensured by continued tectonic uplift along the northern Africa margin, related to the change in motion of
11 the African plate during Early Miocene (Leprêtre et al. 2018 and references therein). The rate of sedimentation
12 was probably important as demonstrated by the existence of water escape and load casts structures.
13 Sedimentation was favored also by the fact that accommodation outpaces the sedimentation rates at the coastline.
14 Tectonic was active during sedimentation as indicated by soft sediment deformations as slumps, ball and pillow
15 and convolutes bedding.

16

17 Conclusion

18

19 This work presents new insight concerning the nature and composition of the sediments, the depositional
20 environments and the factors that have controlled sedimentation for the Eocene-Miocene Mrayt Group in North-
21 Western Rif (Morocco). The petrographic study reveals, for the first time, the mixed siliciclastic/carbonate
22 composition of the deposits and their nomenclature: silty micrites, micritic siltstones, micritic sandstones, sandy
23 micrite, and allochemic sandstones. They reflect sediment supply from an intra-basinal source that provides
24 exoskeletons, glauconitic peloids, algae and rhombohedral crystals of dolomite and mud pebbles and extrabasinal
25 sources, which correspond to the metamorphosed and granitized Paleozoic basement, and its Meso-Cenozoic
26 cover outcropping in the northern African margin. Detrital fraction characteristics indicate also rapid erosion from a
27 young and high relief continental source and a short transport and rapid deposition.

28 Twenty two sedimentary facies that have never been described before are identified, and based on their
29 succession and association a new interpretation of depositional processes and depositional systems are proposed.

30 The paleoenvironments of the Mrayt Group are interpreted as littoral and shallow marine settings: tides-

1 dominated estuary, tides-dominated delta systems and open coast tidal flat, under complex hydrodynamics
2 strongly influenced by river discharge, tidal currents, waves and storms action. Sedimentation occurred in “the
3 Maghrebian basin” under the interplay of: i) tectonics related to the Cenozoic collision of the African and
4 Eurasian continental plates, ii) Cenozoic alternation of warm climate and cooling due to the increasing influence
5 of Antarctica glaciation, iii) sediments supplies induced by rejuvenation of sedimentary sources and iv) sea level
6 fluctuation related to the advance and retreat of ice-sheet on Antarctica.

7 This work brings also additional insights such as the occurrence of Paleodictyon trace fossils in pro-delta
8 environment, Zoophycos trace fossils in nearshore settings and Cruziana burrow in the intertidal zone. The
9 first two trace fossils are normally associated with deep-sea flysch settings and Cruziana is considered typical of
10 subtidal above storm wave base. In addition to these new findings, this work is important for increasing our
11 knowledge about ancient tides dominated deltas that is less investigated in comparison to the other deltaic
12 systems (waves or river dominated) and its responses to sea level changes and tectonics. Furthermore, this work
13 is also important for documenting an example of mixed siliclastic/ carbonate in nearshore to shallow depositional
14 setting. Last but not least, it consists an essential contribution for a better knowledge of North Western Rif belt and
15 the the peri-Mediterranean alpine chain.

16

17 **Acknowledgements** Authors wish to thank: Beatriz Bádenas, Assistant Editor for her rigorous evaluation and for
18 her corrections and advices,

- 19 - the two anonymous reviewers for useful comments and suggestions,
- 20 - Julian Tejera de Leon for showing us the outcrops of the Mrayt Group.

21

22 **References**

23

24 Abdelkhaliki L (1997) Evolution tectono-sédimentaire des dépôts gravitaires dans le Prérif interne et l'unité
25 du Habt (Rif externe occidentale, Maroc) : mise en place dans les bassins néogènes d'avant-fosse. Thèse 3ème
26 cycle, Univ. Md V, Rabat, 176 p

27 Allen P, Homewood P (1984) Evolution and mechanics of a Miocene tidal sandwave: *Sedimentology*, v.
28 31: 63- 81

29 Andrieux J (1971) La structure du Rif central. Etude des relations entre la tectonique de compression et les
30 nappes de glissement dans un tronçon de la chaîne alpine. Notes et Mém. Serv. Géol., Maroc, 235

1 Belghouthi F, Wetzel A, Zouari E, Jeddi RS (2020) Zoophycos in storm affected Maastrichtian deposits (N
2 Tunisia) Ichnos 27

3 Boersma J R (1969) Internal structure of some tidal mega-ripples on a shoal in the Westerschelde estuary,
4 the Netherlands: report of a preliminary investigation. Geol. Minjnb, Amsterdam, 48: 409-414

5 Boggs S (1995) Principles of Sedimentology and Stratigraphy, 2nd Edition. PrenticeHall Inc.

6 Bouillin J (1986) Le "bassin maghrebin"; une ancienne limite entre l'Europe et l'Afrique a l'ouest des
7 Alpes. Bulletin de la SocieteGeologique de France, vol.II, issue.4, 547-558

8 Brinkhuis H, Schouten S, Collinson ME, Sluijs A, Damsté JSS, Dickens GR, Huber M, Cronin TM,
9 Onodera J, Takahashi K, Bujak JP, Stein R, Van der Burgh J, Eldrett JS, and the Expedition 302 Scientists (
10 2006)Episodic fresh surface waters in the Eocene Arctic Ocean: Nature, v. 441, no. 7093, p. 606-609.

11 Buatois L, Mangano M G (2011) Ichnology: Organism-Substrate Interactions in Space and Time.
12 Geological Magazine , 149 : Issue 4 , pp. 750.

13 Cazzola C, Critellis S (1987)Litostratigraphia e petrologia delle quarzoarenitorbidicheoligomioceniche di
14 Asilah (Catenadel Rif, Marocco nord-occidentale). Miner.Petrogr.Acta XXX: 203-226

15 Chiarella D, Longhitano S.G, Tropeano M (2017) Types of mixing and heterogeneities in siliciclastic-
16 carbonate sediments,Marine and Petroleum Geology, 88 (12): 617-62

17 Collinson (1969) The sedimentology of the Grindslow shales and the Kinderscout grit; a deltaic complex in
18 the Namurian of northern England , Journal of Sedimentary Research 39 (1): 194–221

19 Daidu F (2012) Principles of Tidal Sedimentology, Ed. Springer,187-222

20 Dalrymple RW (1992) Tidal depositional systems. In: Walker, R.G., James, N. P., (eds). Facies Models:
21 Response to Sea LevelChange. Geological Association of Canada, St. John's, 195-218.

22 Dalrymple RW, Knight RJ, Lambiase JJ (1978) Bedforms and their hydraulic stability relationships in a
23 tidal environment, Bay of Fundy, Canada. Nature, 275: 100-104

24 Dalrymple RW, Makino Y (1989) Description and genesis of tidal bedding in the Cobequid Bay–Salmon
25 river estuary, Bay of Fundy, Canada. In: Taira, A., Masuda, F. (Eds.), Sedimentary Facies of the active Plate
26 Margin. Terra Publishing, Tokyo: 151 – 177

27 Dalrymple RW, Zaitlin BA, Boyd RA (1992) A conceptual model of estuarine sedimentation. J Sediment
28 Petrol 62:1130–1146.

1 Dalrymple RW, Mackay D A, Ichaso A A, Choi K S (2012) Processes, Morphodynamics, and Facies of
2 Tide-Dominated Estuaries. In R.A. Davis, Jr. and R.W. Dalrymple (eds.), Principles of Tidal Sedimentology, 79.
3 Springer Science and Business Media B.V. 2012

4 De Boer P, Oost A, Visser MJ (1989) The Diurnal Inequality of the Tide as a Parameter for Recognizing
5 tidal Influences. *Journal of Sedimentary Petrology* 59: 912-921

6 De Raaf JFM, Boersema JR, Van Gelder A (1977) Waves-generated structures and sequences from a
7 shallow marine section, lower Carboniferous, County Cork, Ireland. *Sedimentology* 24: 451- 483

8 Dewey JF, Helman ML, Knott SD, Hutton DHW (1989) Kinematics of the western
9 Mediterranean. *Geological Society London Special Publications* 45 (1): 265-283

10 Dickinson WR, Rich EI (1972) Petrologic intervals and petrofacies in the Great Valley Sequence,
11 Sacramento Valley, California: *Geol. Soc. America Bull* 83: 3007–3024

12 Durand-Delga M, Hottinger L, Marcáis J, Mattauer M, Milliard Y, Suter G (1962) Données nouvelles sur la
13 structure du Rif. *Mém. h. sér. Soc. géol., France* 399- 422

14 Frey RW, Howard J D, Pryor WA (1978) Ophiomorpha: its morphologic, taxonomic, and environmental
15 significance. *Palaeogeogr., Palaeoclimatol., Palaeoecol.* 23: 199- 229.

16 Fürsich F, Taheri J, Wilmsen M (2007) New occurrences of the trace fossil *Paleodictyon* in shallow marine
17 environments: Examples from the Triassic-Jurassic of Iran. *Palaios.* 22: 408-416.

18 Galloway WE (1975) Process framework for describing the morphologic and stratigraphic evolution of
19 deltaic depositional systems. In: Broussard ML (ed) *Deltas: models for exploration*. Houston Geological Society,
20 Houston, 87–98

21 Guiraud R, Bosworth W, Thierry J, Delaplanque A. (2005) Phanerozoic geological evolution of northern
22 and central Africa: an overview. *Journal of African Earth Sciences* 43, 83–143.

23 Goodbred S L jr, Saito Y (2012) Tide-Dominated Deltas. R.A. Davis, Jr. and R.W. Dalrymple (eds.),
24 Principles of Tidal Sedimentology, 129, Springer Science.

25 Hamoumi N (1995a) Réinterprétation des contacts situés entre les unités des flyschs du Déroit de Gibraltar
26 et de sa rive sud -Intérêt des études sédimentologiques et géophysiques pour le Projet Liaison Fixe Europe-
27 Afrique. Actes du IV Coloquio Internacional sobre el Enlace Fijo Estrecho de Gibraltar, Tomo II El Medio
28 Fisico, SNED & SECEG Edit., pp. 217- 224

1 Hamoumi N (1995b) Les ensembles géologiques de subsurface dans la région du Puits Malabata : Etude
2 sédimentologique et géochimique- Essai de corrélation Actes du IV Coloquio Internacional sobre el Enlace Fijo
3 Estrecho de Gibraltar, Tomo II El Medio Fisico, SNED & SECEG Edit., pp. 225- 247

4 Hamoumi N, Salhi F, Ouldchalha A (1995) L'Oligo-Miocène de la rive sud du Déroit de Gibraltar (Rif-
5 Maroc) : Faciès et environnements sédimentaires, contrôle géodynamique et eustatique. Actes du IV Coloquio
6 Internacional sobre el Enlace Fijo Estrecho de Gibraltar, Tomo II El Medio Fisico, SNED & SECEG Edit., pp.
7 21- 50

8 Haq BU, Hardenbol J, Vail PR (1987) Chronology of fluctuating sea levels since the Triassic (250 million
9 years ago to present).Science 235: 1156–1166.

10 Harms JC, Southard JB, Spearing DR, Walker RG (1975) Depositional environments as interpreted from
11 primary sedimentary structures and stratification sequences. Soc. Econ. Paleont. Mineral., Short Course 2, Dallas

12 Howard JD, Reineck HE (1981) Depositional Facies of High-Energy Beach-to-Offshore Sequence:
13 Comparison with Low-Energy Sequence. American Association of Petroleum Geologists Bulletin, 65: 807-830

14 Jelby ME, Grundvåg SA, Helland-Hansen W, Olausen S, Stemmerik Lars (2019) Tempestite facies
15 variability and storm-depositional processes across a wide ramp: Towards a polygenetic model for hummocky
16 cross-stratification.Sedimentology:10.1111.

17 Knaust D (2004) Cambro-Ordovician trace fossils from the SWNorwegian Caledonides. Geological
18 Journal. 39: 1 – 24.

19 Kreisa RD, Moiola RJ (1986) Sigmoidal tidal bundles and other tide-generated sedimentary structures of
20 the Curtis Formation. Geological Society of America Bulletin (97) 4: 381-387

21 Leprêtre R, Frizon de Lamotte D, CombierV, Gimeno-Vives O, Mohn G, Eschard R (2018) The Tell-Rif
22 orogenic system (Morocco, Algeria, Tunisia) and the structural heritage of the southern Tethys margin. BSGF -
23 Earth Sciences Bulletin, 189, 10.

24 Lowe DR (1975) Water escape structures in coarsegrained sediments. Sedimentology, 22: 157-204

25 Mansfield GR (1971) Origin of the Brown Mountain light in North Carolina, Geological Survey (U.S.): 18,
26 647

27 Metz R (2012) The Trace Fossil Paleodictyon within The Cruziana Ichnofacies: First Record from The
28 Devonian in Pennsylvania. Ichnos19: 10.1080

1 Mowbray T, Visser M (1984) Reactivation surfaces in subtidal channel deposits, Oosterschelde, Southwest
2 Netherlands. *Journal of Sedimentary Petrology*, 54 (3): 811–824

3 Mutti E (1985) Turbidite Systems and Their Relations to Depositional Sequences. In Zuffa G. G. ed.
4 Provenance of arenites Dordrecht, D. Reidel Publishing Company, 65–93

5 Miall A D (1992) Alluvial deposits Facies models, response to sea level change. In: Walker RG, James N P,
6 (eds). *Facies Models: Response to Sea Level Change*. Geological Association of Canada, St. John's, 119-142

7 Morley CK (1992) Tectonic and sedimentary evidence for synchronous and out-of-sequence thrusting,
8 Larache-Acilah area, western Moroccan Rif. *J. Geol. Soc., London*, 149: 39- 49

9 Mount JF (1985) Mixed siliciclastic and carbonate sediments: a proposed first-order textural and
10 compositional classification. *Sedimentology*, 32: 435-442

11 Nesbitt E A, Campbell K A (2006) The Paleoenvironmental Significance of *Ptilonichnus*. *PALAIOS* 21 (2):
12 187–196.

13 Nio SD, Yang CS (1989) Recognition of tidally-influenced Facies and Environments. *International*
14 *Geoservices BV*, 230

15 Ouldchalha A, Hamoumi N, Salhi F (1995) Les flyschs d'âge éocène de la Rive sud du Déroit de Gibraltar
16 (Rif, Maroc) : Faciès et environnements sédimentaires, contrôle géodynamique et eustatique. *Actes du IV*
17 *Coloquio Internacional sobre el Enlace Fijo Estrecho de Gibraltar, Tomo II El Medio Fisico, SNED & SECEG*
18 *Edit., pp. 339- 350*

19 Odin G S (1985) Significance of green particles (glaucony, berthierine, chlorite) in arenites. In *Provenance*
20 *of arenites, GG Zuffa (Ed.), NATO ASI Series, V 148:279-307*

21 Pandey DK, Uchman A, Kumar V, Shekhawat RS (2014) Cambrian trace fossils of the Cruziana ichnofacies
22 from the Bikaner-Nagaur Basin, north western Indian Craton. *Journal of Asian Earth Sciences*, 81: 129–141

23 Pettijohn FJ, Potter PE, Siever R (1973) *Sand and Sandstone* pp. 617, Springer-Verlag, Berlin

24 Platt JP, Vissers RLM (1989) Extensional collapse of thickened continental lithosphere: A working
25 hypothesis for the Alboran Sea and Gibraltar arc. *Geology* 17, 540-543

26 Raissouni A, Raïbi F, Tejera De Leon J, Dakki M (2008) Les Grès de Mrayt : un environnement de
27 plateforme externe soumis à l'action des houles de tempête. *Evolution de l'Eocène au Miocène moyen (Rif Nord*
28 *occidental)*. 20ème Colloque Bassins sédimentaires Marocains, Oujda

1 Reading HG (1986) *Sedimentary Environments and Facies*. Blackwell Scientific Publications, Oxford, 471-

2 519

3 Reineck H E (1969) Die Entstehung von Runzelmarken. *Nat. Mus.* 99: 386-388

4 Reineck HE, Singh IB (1980) *Depositional Sedimentary Environments*, Springer-Verlag, Berlin,

5 Heidelberg, New York

6 Salhi F, Hamoumi N, Oueddchalha A (1995) Les flyschs d'âge crétacé de la rive sud du Déroit de Gibraltar

7 (Rif-Maroc): Faciès et environnements sédimentaires, contrôle géodynamique et eustatique. Actes du IV

8 Coloquio Internacional sobre el Enlace Fijo Estrecho de Gibraltar, Tomo II El Medio Físico (SNED & SECEG

9 Edit.), pp. 361- 375

10 Shahin D, Murray G, Maceachern J (2009) Tidally Modulated Shorefaces. *Journal of*

11 *Sedimentary Research*. 79: 793-807

12 Seilacher A (1967) Bathymetry of trace fossils. *Marine Geology*, 5:4, 13- 42

13 Srivastava S, Schouten H., Roest W, Klitgord K., Kovacs L., Verhoef J, Macnab R (1990) Iberian Plate

14 kinematics: a jumping plate boundary between Eurasia and Africa. *Nature*

15 Suter G, Fiechter G (1966) Le Rif méridional atlantique (Maroc) : aperçu structural sur la région Ouezzane-

16 Zoumi et le pays du Habt (Larache). *Notes Mém. Serv. Géol. Maroc* (26) 188: 15-20

17 Suter G (1980) Carte géologique de la chaîne rifaine au 1/50 000. *Notes Mém. Serv. Géol. Maroc* 245a & b

18 Suter G (1986) Carte géologique de la chaîne rifaine au 1/50 000. *Notes Mém. Serv. Géol. Maroc* 346

19 Swezey CS (2009) Cenozoic stratigraphy of the Sahara, Northern Africa. *Journal of African Earth Sciences*

20 53 89–121

21 Swift DJP, Figueiredo Jr, Freeland G, Oertel GF (1983) Hummocky Cross-Stratification and Megaripples:

22 A Geological Double Standard? *Journal of Sedimentary Petrology*, 53 :1295-1317

23 Tejera de Leon J (1993) Les bassins néogènes d'avant-pays du Rif externe occidental liés à la

24 transformante Jebha-Arbaoua (Maroc). Thèse Doct. Etat. es Sciences, Univ. de Pau et des Pays de l'Adour 323 p.

25 Terwindt JHJ (1981) Origin and sequences of sedimentary structures in mesotidal deposits of the North

26 Sea. *Spec. Publ. Int. Assoc. Sedimentol.* 5: 4–26

27 Tessier B, Monfort Y, Gigot P, Larsonneur C (1989) Enregistrement des cycles tidaux en accréation

28 verticale, adaptation d'un outil de traitement mathématique. Exemples en baie du Mont-Saint-Michel et dans la

29 molasse marine miocene du bassin de Digne. *Bull. Soc. Géol. Fr.* 8: 1029-1041

1 Visser MJ (1980) Neap-spring cycles reflected in Holocene subtidal large-scale bedform deposits. A
2 preliminary note. *Geology*, 8: 543-546

3 Wildi W (1983) La chaine tello-rifaine: Structure, Stratigraphie et évolution du Trias au Miocène. *Revue de*
4 *Géologie dynamique et de Géographie Physique*, 24, 201-297

5 Wright LD, Short AD (1984) Morphodynamic variability of surf zones and beaches: A synthesis, *Marine*
6 *Geology*, 56: Issues 1–4, 93-118

7 Wright LD, Friedrichs C (2006) Gravity-driven sediment transport on continental shelves: A status report,
8 *Continental Shelf Research - CONT SHELF RES*, 26: 2092-2107

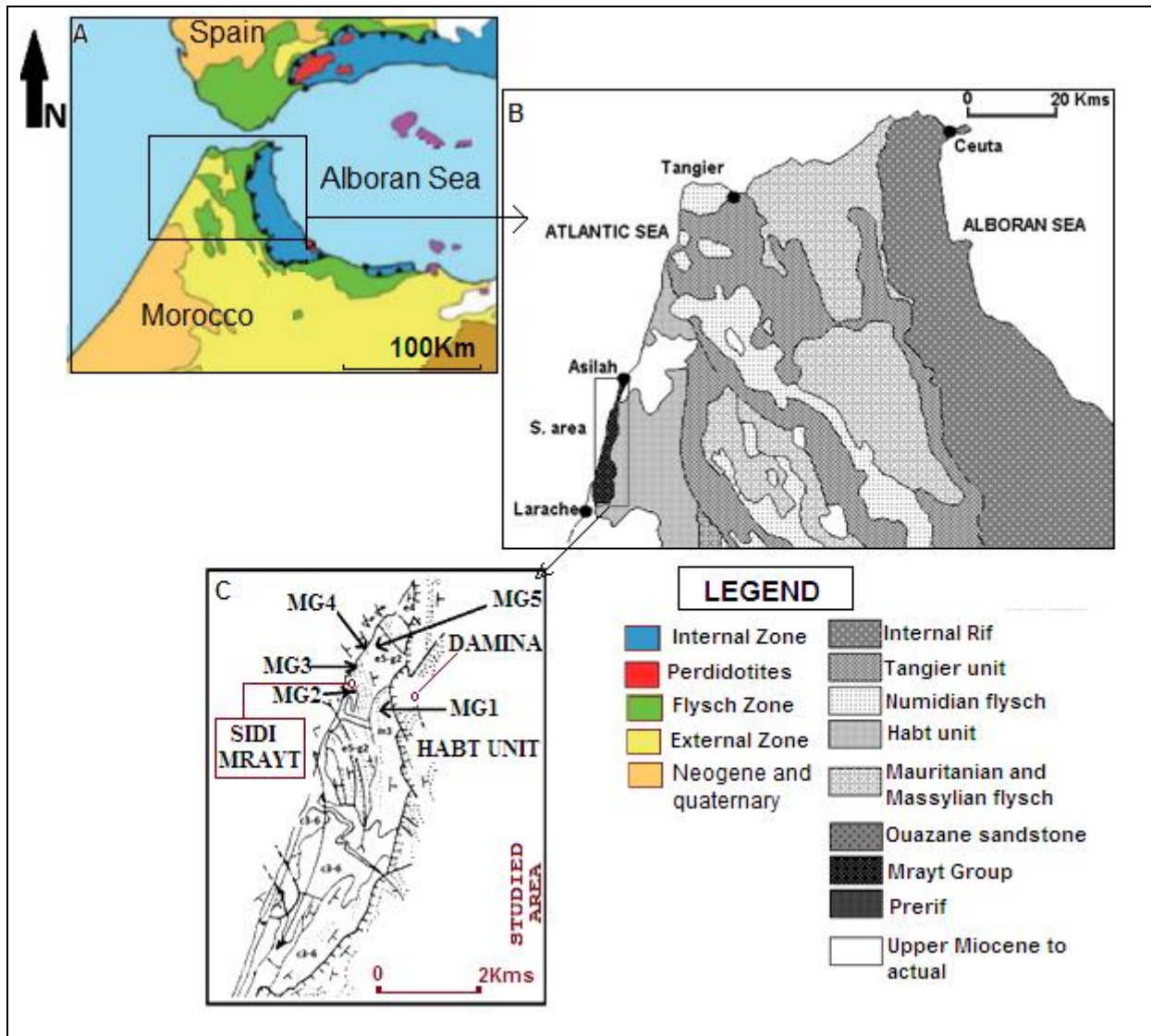
9 Yang BC, Dalrymple R, Chun SS (2006) The Significance of Hummocky Cross-Stratification (HCS)
10 Wavelengths: Evidence from an Open-Coast Tidal Flat, South Korea. *Journal of Sedimentary Research*, 76: 2-8.

11 Zachos JM, Pagani L, Sloan E, Thomas K., Billups K (2001) Trends, Rhythms, and Aberrations in Global
12 Climate 65 Ma to Present. *Science*, 292, Issue 5517, 686-693.

13 Zhang LJ, Zhao Z (2016) Complex behavioural patterns and ethological analysis of the trace fossil
14 *Zoophycos*: evidence from the Lower Devonian of South China. *Lethaia* 49:275–284.

15
16
17
18
19
20
21
22
23
24
25
26
27
28
29
30

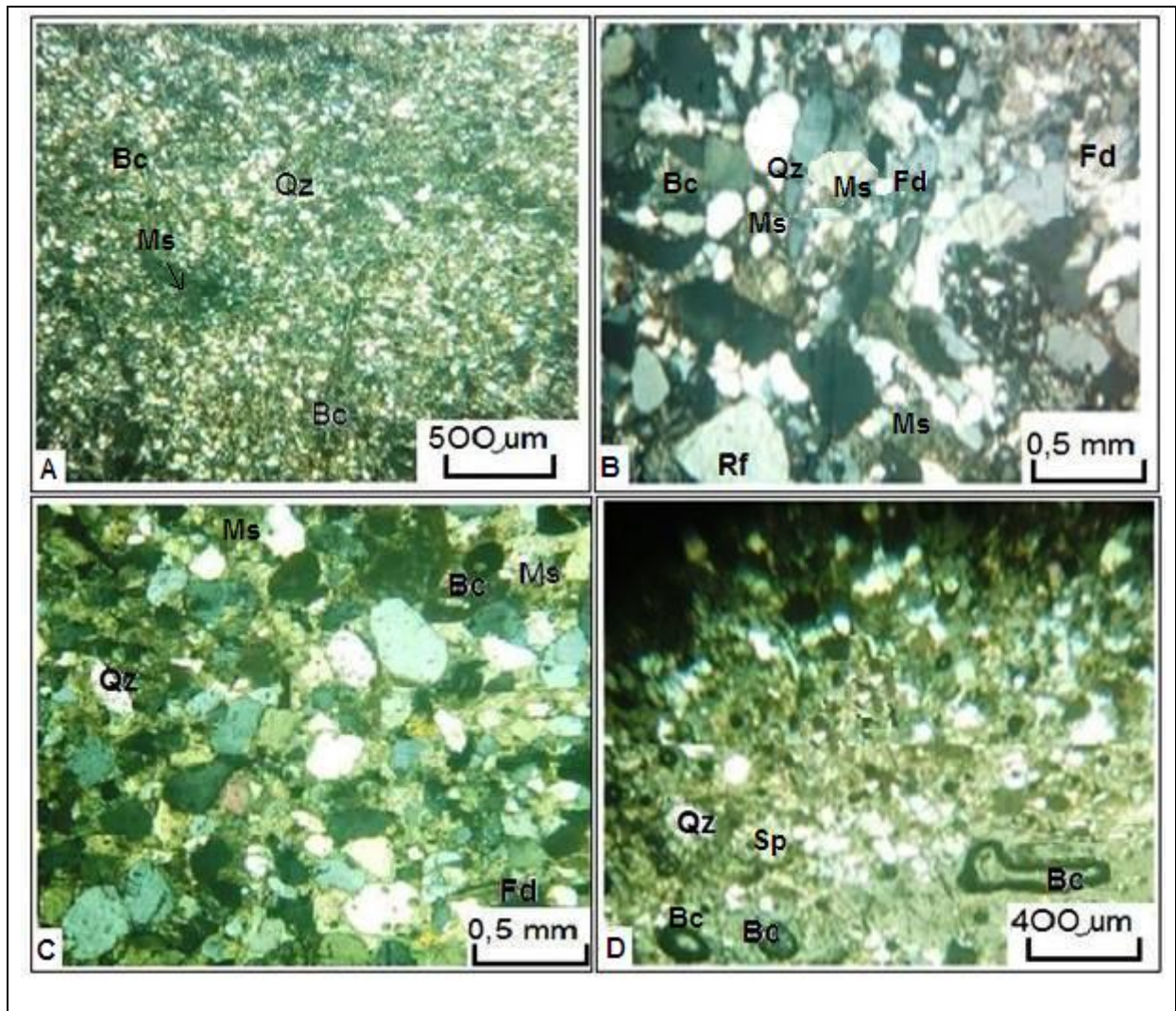
1 Fig. 1



2
 3 A geological map of the geological domains in the Betic–Rif orogenic system (after Platt and Vissers 1989); B Location of
 4 the Mrayt Group outcrops in the geological map of the North Western Rif (after Suter 1980); C Location of the studied
 5 outcrops in the structural map of Suter (1980): MG1- Damina section, 80m thick (X= 6.06; Y= 35.42), MG2- Marabout
 6 section, 750m thick (X= 5.85; Y= 35.36), MG3- Sidi Mrayt beach section, 200m thick (X= 5.85; Y= 35.41), MG4- Merja
 7 section, 520m thick (X= 5.96; Y= 35.43), and MG5- Merja ravine section, 280m thick (X= 6.05; Y= 35.44). S. area: Studied
 8 area

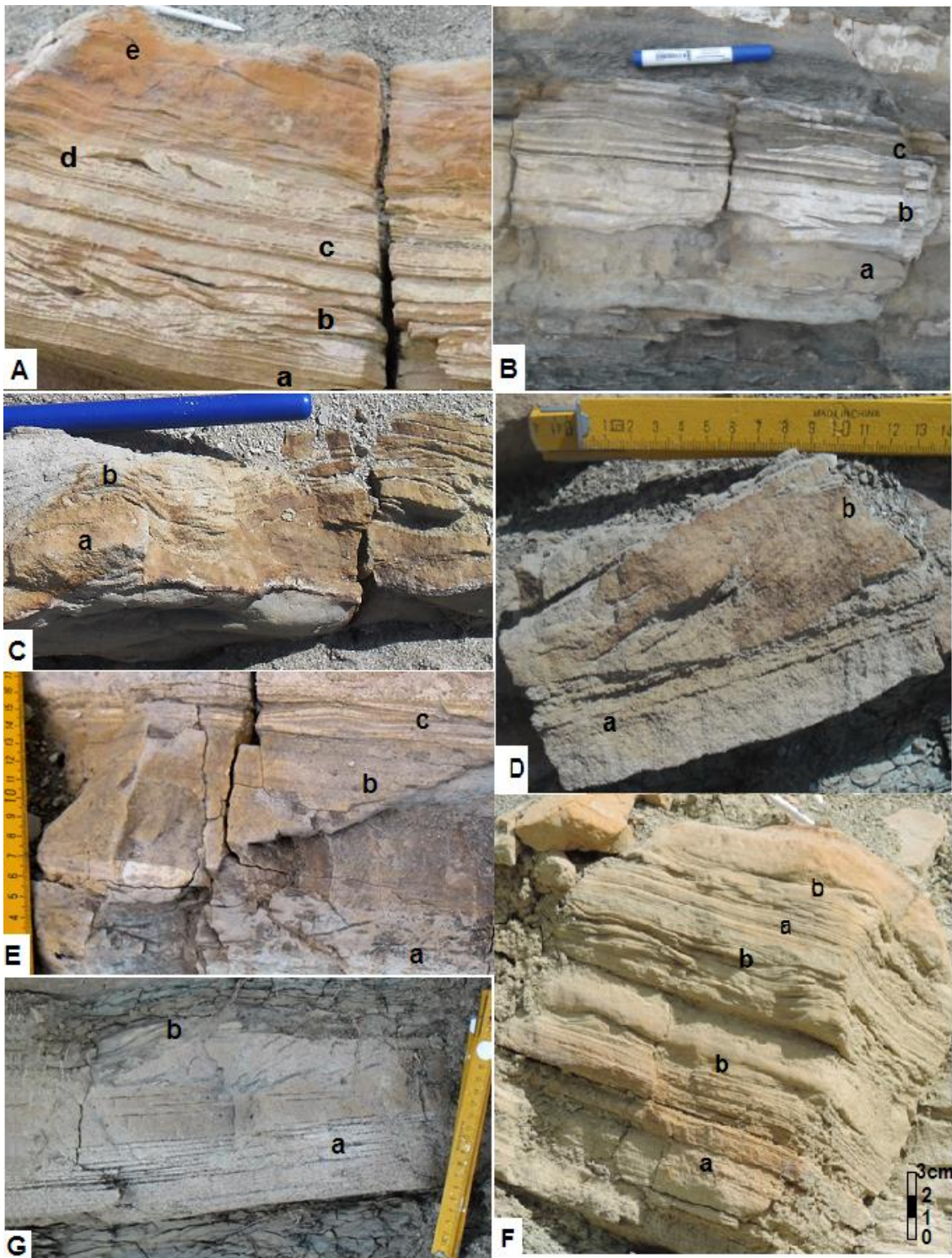
9
 10
 11
 12
 13
 14

1 Fig. 2

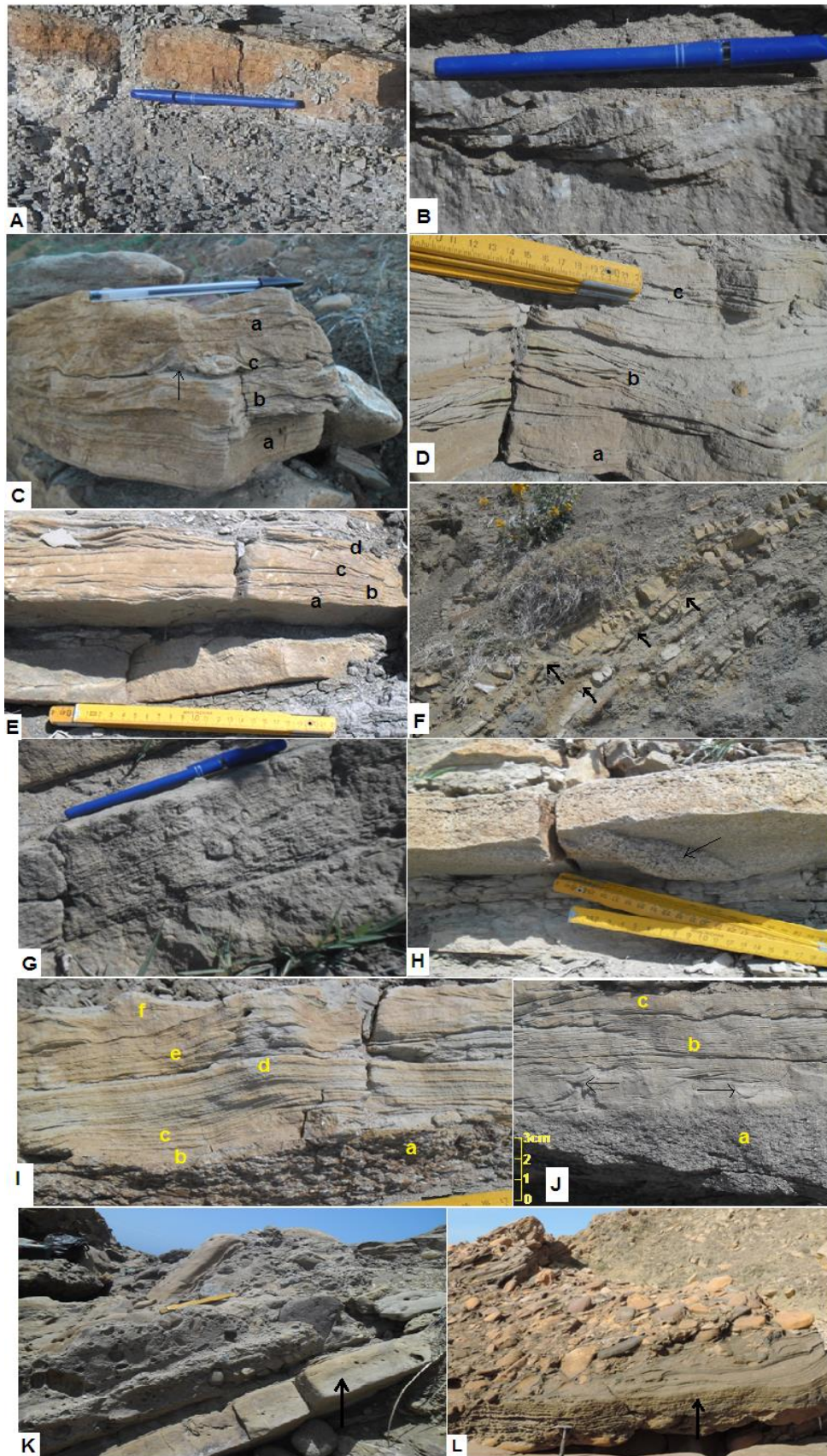


Petrofacies of the Mrayt Group: A- micritic siltstone; B- sandy micrite; C- micritic sandstone; D- sandy allochemic sandstone. Bc- Bioclasts, Qz- Quartz, Sp- Sparite, Ms- microsparite, Fd- fedspath, Rf- Rock fragment

1 Fig. 3



2
 3 Sedimentary facies. A- Facies F1 (a and c- mud couplets, b-flaser bedding, d- wavy bedding, e-lenticular bedding). B- Facies F2
 4 (a and c- mud couplets, b-flaser bedding, c- asymmetrical ripples); C- Facies F3 (a- slightly deformed level without visible
 5 bedding, b- asymmetrical ripples); D- Facies F4 (a- parallel undulated plane laminations, b- tangential oblique laminations); E-
 6 Facies F5 (a- mud pebbles, b- massive level, c- parallel undulated lamination); F- Facies F6 (a- rhythmic parallel laminations, b-
 7 tidal bundles); G- Facies F7 (a- tidal rhythmites, b- tidal bundles)

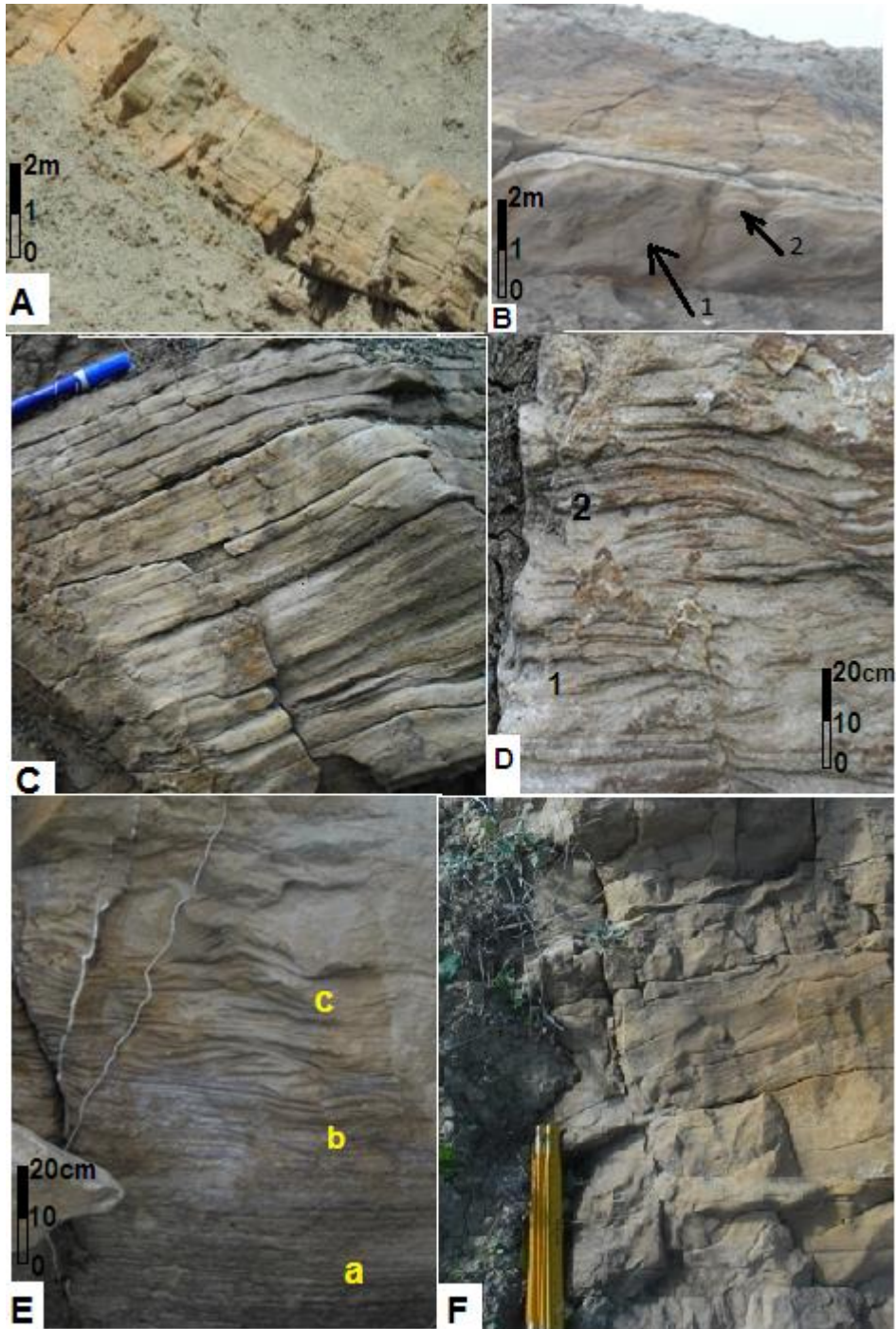


1

2 **Fig.4** Sedimentary facies. A- Facies F8; B- Facies F9; C- Facies F10 (a- mud couplets, b- sigmoidal bundles, c- symmetrical
 3 ripples, arrows indicate flame structures); D- Facies F11 (a- tidal bindles, b-cross laminated beds, c- tidal rhythmites; E- Facies

1 F12 (a- asymmetrical ripples, b- tidal rhythmites, c- cross laminated beds , d- tidal bundles); F- Facies F13 (arrows indicate
 2 hummocks); G- detail of F13: Hummocky cross stratification; H- Facies F14 (arrows indicate flute cast); I- Facies F15 (a-
 3 microconglomerate, b- massive level, c- asymmetrical ripples, d- tidal rhythmites, e- tidal bundles, f- asymmetrical ripples); J-
 4 Facies F16 (a- microconglomerate, b- tidal rhythmites, c- tidal bundles, arrow indicate convolute bedding); K- Facies F17 a and b
 5 (arrow indicate medium to fine -grained sandstone bed); L- Facies F17c (arrow indicate coarse sandstone bed)

6
 7 **Fig. 5**

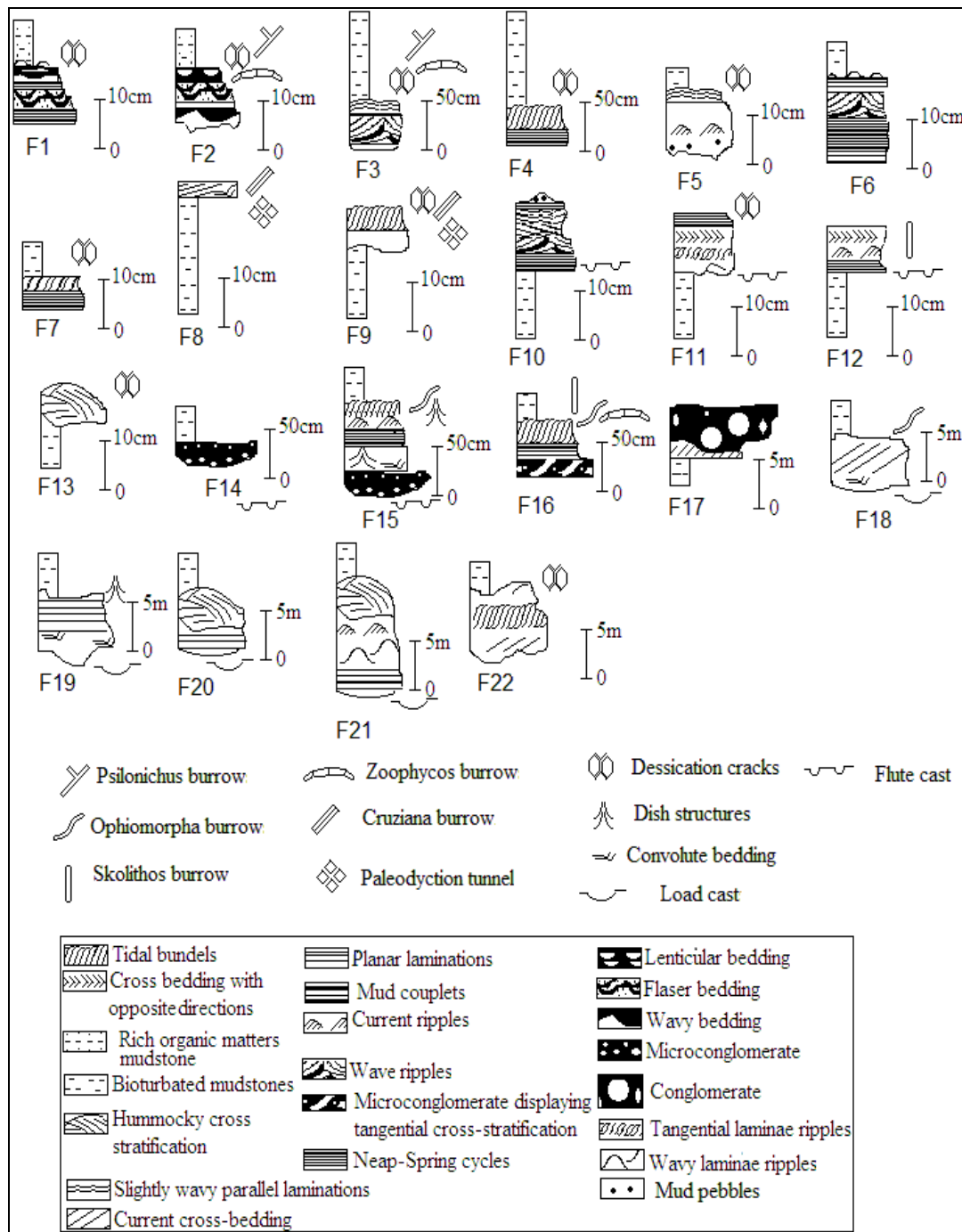


8

1 Sedimentary facies. A- Low-angle cross lamination in Facies F18; B- Load casts (arrows 1: large-scale and 2: small-scale) at
 2 the base of Facies F18; C- Facies F19; D- Facies F20 (1- planar parallel lamina and 2- Hummocky cross stratification); E-
 3 Facies F21 (a- tidal rhythmites, b- symmetrical wave ripples passing to megaripple cross bedding, c- micro-hummocky cross
 4 stratification); E- Facies F21 (a- tidal rhythmites, b- symmetrical wave ripples passing to megaripple cross bedding, c- micro-
 5 hummocky cross stratification); F- Facies F22

6

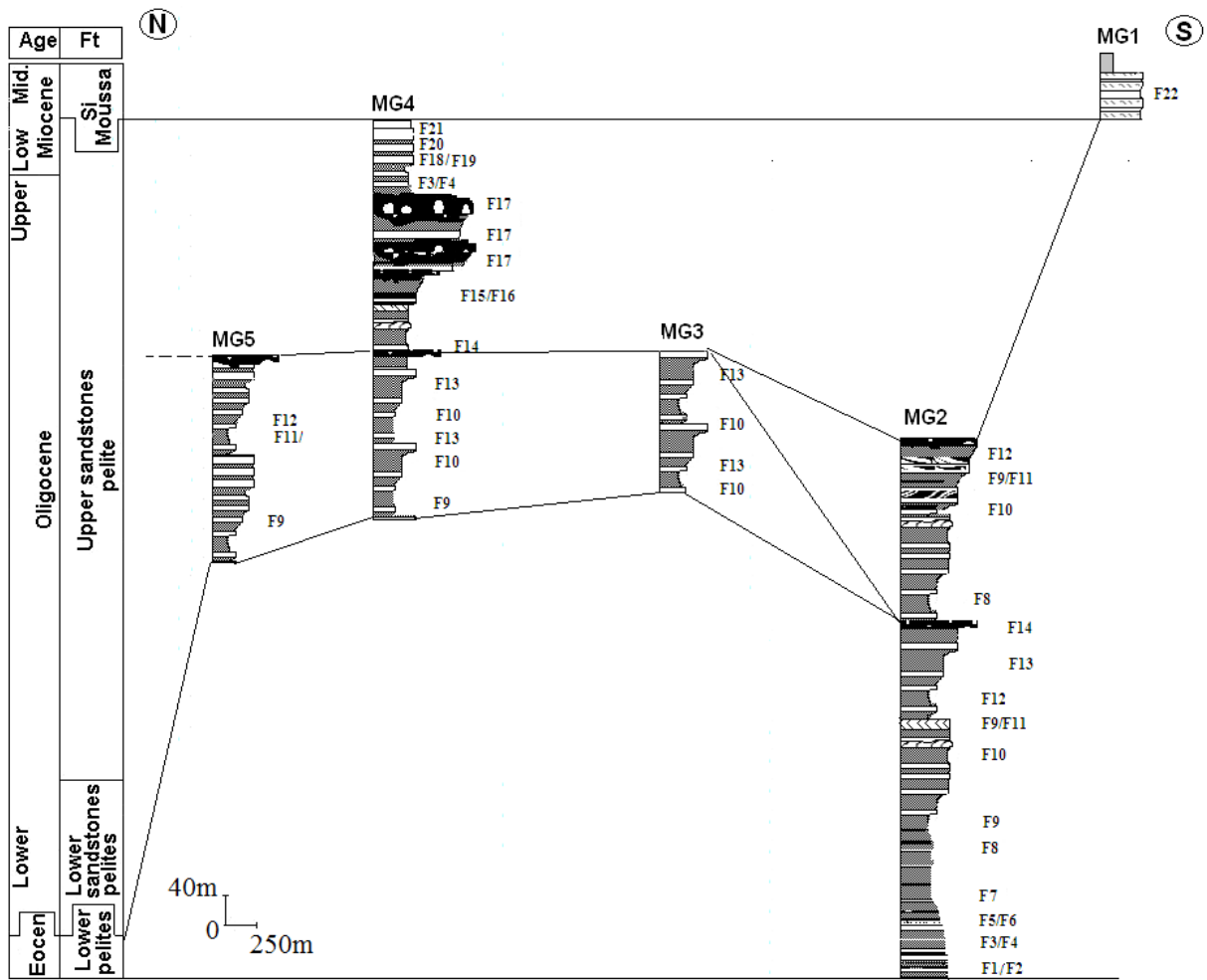
7 **Fig. 6**



8

9 Facies of the Mrayt Group

1 Fig. 7



2

3 Studied outcrops from the Mrayt Group: MG1- Damina section, MG2- Marabout section, MG3- Sidi Mrayt beach section, MG4-

4 Merja section, and MG5- Merja ravine section (See locations in Fig.1C)

5

6

7

8

9

10

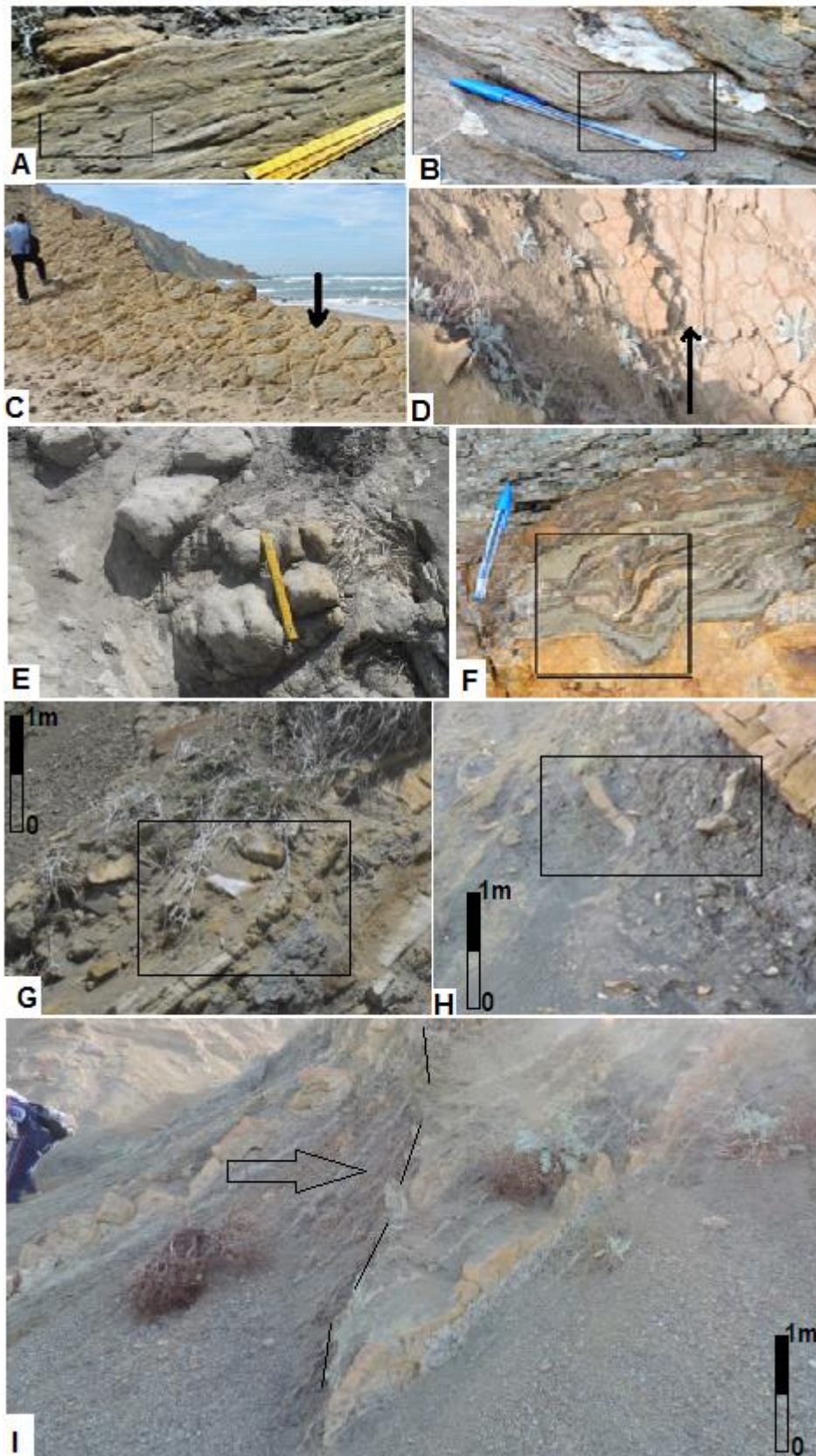
11

12

13

14

1 Fig. 8

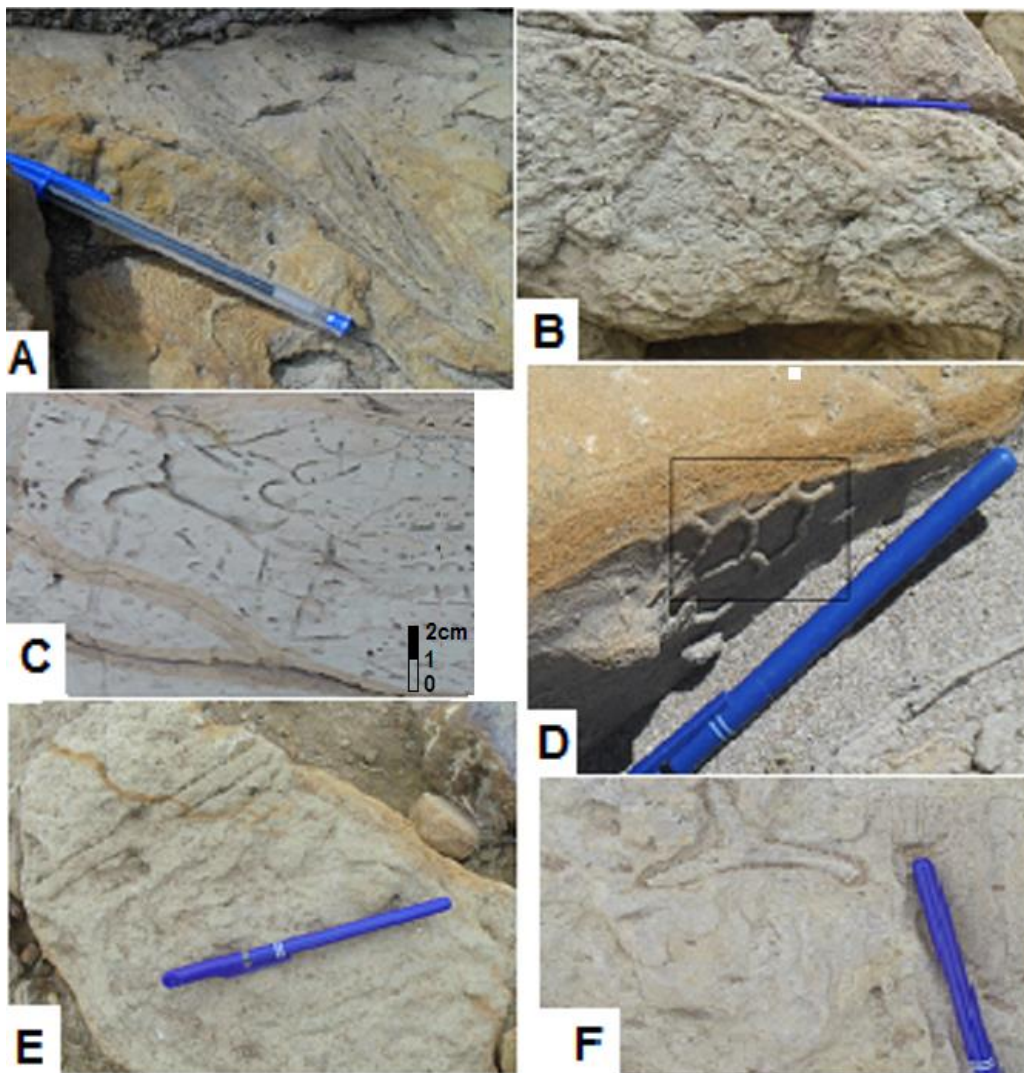


2

1 Sedimentary structures. A- Flute casts (F10, observed also in F1, F11, F12, F14 and F15); B- dish and pillar structures (F15,
 2 observed also in F19); C- large scale desiccation cracks observed in F3 in the upper pelites formation; D- cm to dm desiccation
 3 cracks (F11, observed also in F1, F2, F3, F4, F5 F7, F9, F13 and F22); E-ball and pillow (F16, observed also in F20); F-
 4 convolutes bedding (F15, observed also in F8, F16, F18, and F19); G-synsedimentary deformations in the lower pelites
 5 formation; H- synsedimentary deformations in the lower sandstones formation; I- synsedimentary deformations in the upper
 6 pelites formation (dashes show synsedimentary tectonics)

7

8 **Fig. 9**



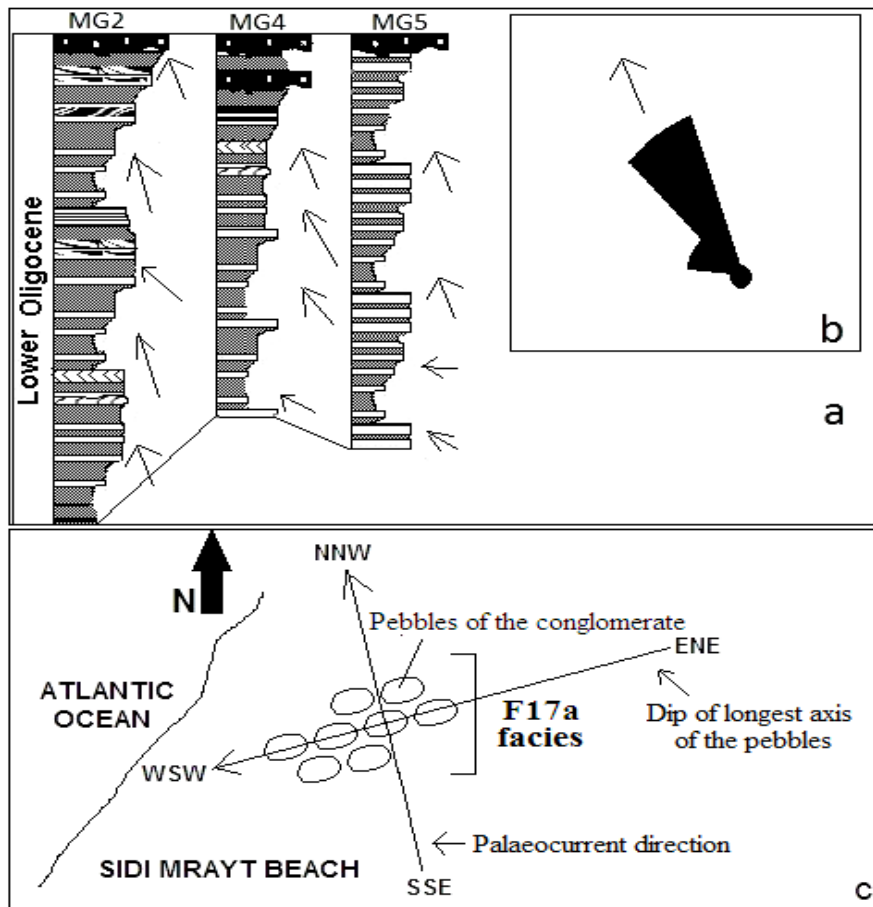
9

10 Trace fossils. A- Zoophycos burrow (F12); B- Ophiomorpha burrow (F10, observed also in F12, F13 and F16); C- Skolithos
 11 burrow (F12, observed also in F13); D- Palaeodictyon tunnel (F4); E- Cruziana burrow; F- Psilochinus burrow

12

13

1 Fig. 10



2

3 Palaeocurrent measurements (a) and the rose diagram (b) (main direction SSE to NNE, n=48). MG2- Marabout delta, MG4-
4 Merja delta, and MG5- Merja ravine delta (locations in Fig.1C), dip of longest axis of pebbles (c)

5

6

7

8

9

10

11

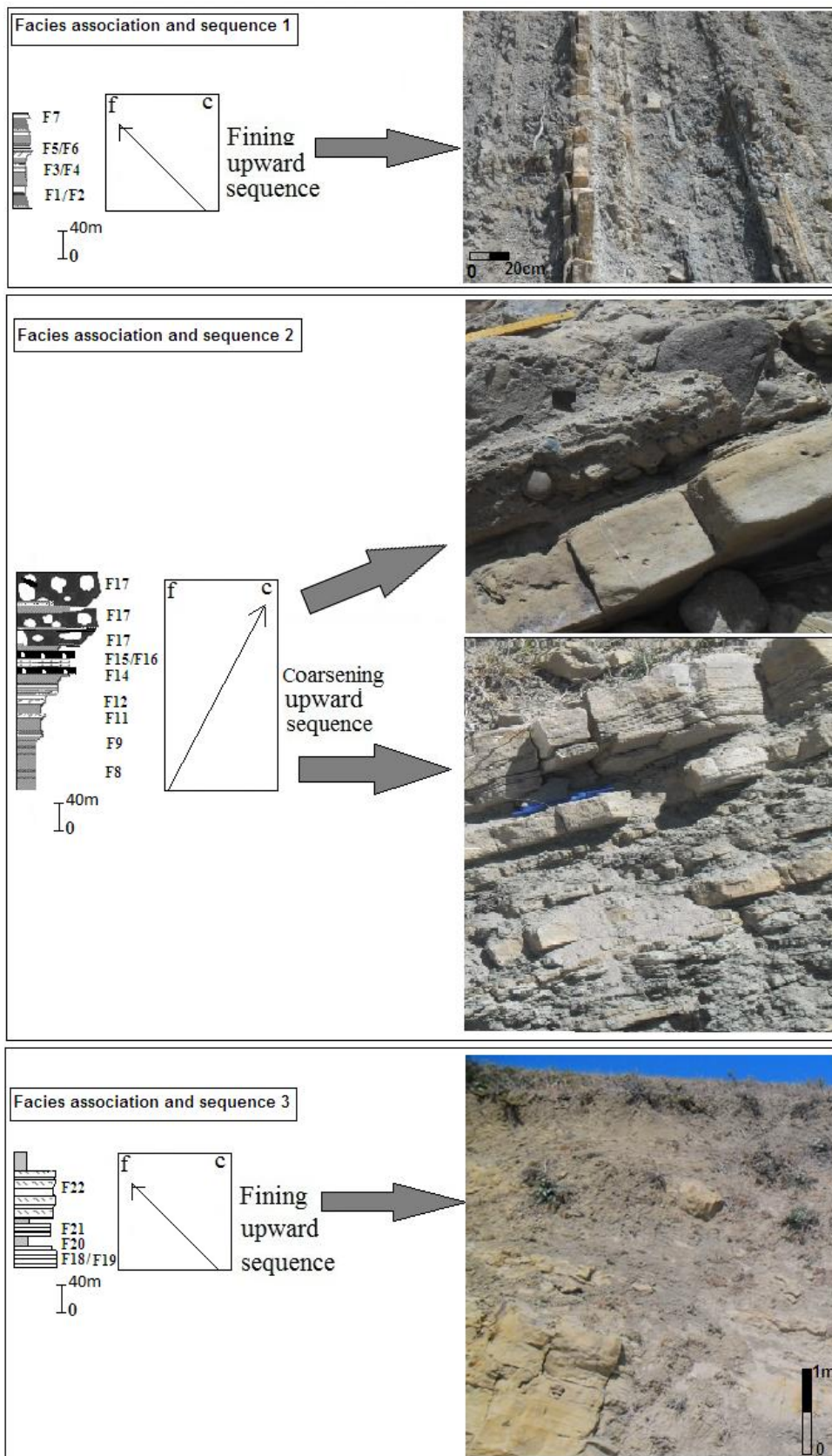
12

13

14

15

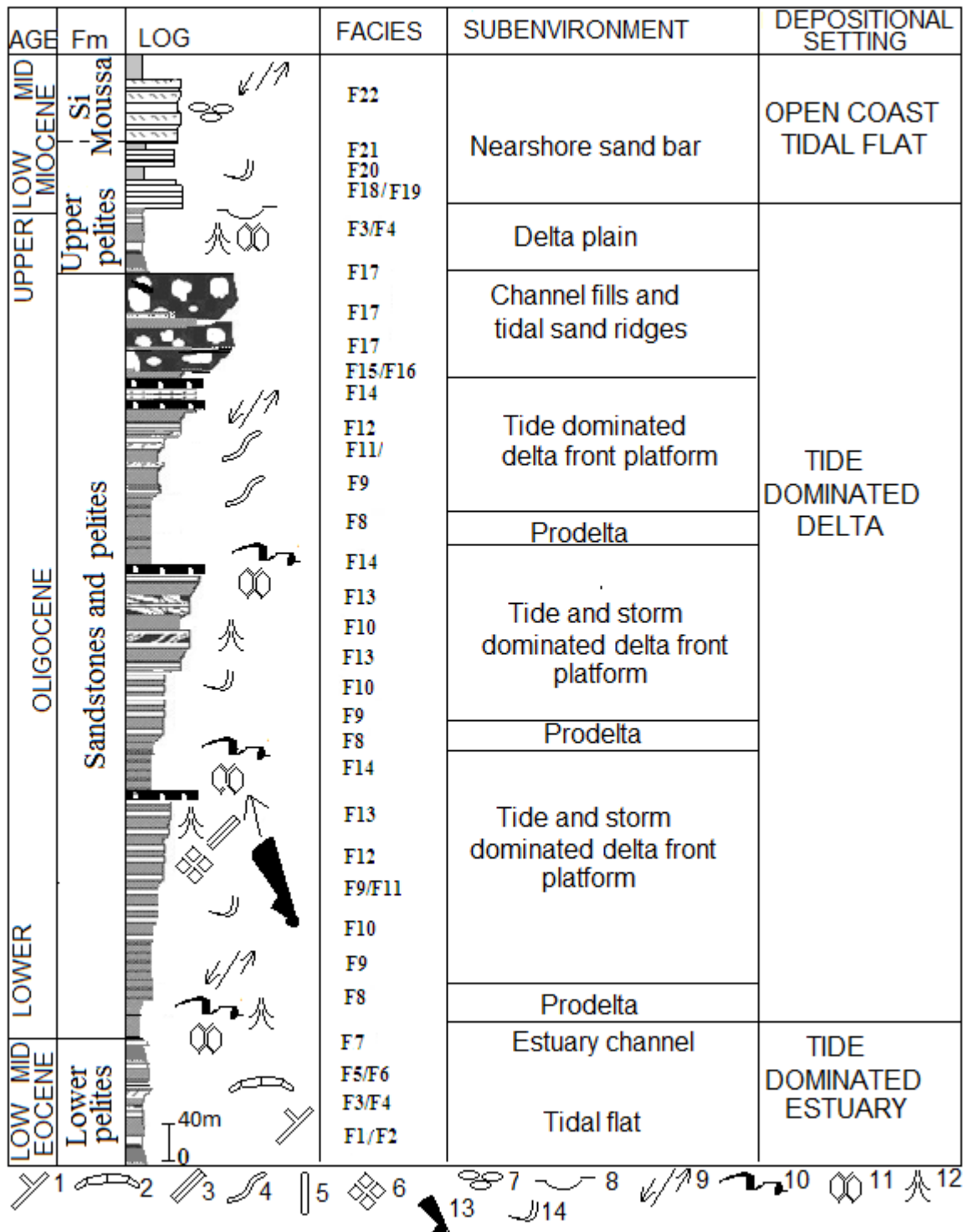
1 Fig. 11



2

3 Facies associations and sequences of the Mrayt Group. f: fine grained sediment. c: coarse grained sediment

1 Fig. 12



2
3 Lithology, sedimentary environments and depositional sequences of Mrayt Group (1- Pylonichus burrows, 2-Zoophycos
4 burrows, 3- Cruziana burrows, 4- ophiomorpha burrows, 5- skolithos burrows, 6- Paleodictyon tunnels, 7- ball and pillow, 8- load
5 cast, 9- synsedimentary fault, 10- convolute bedding, 11- dessication cracks, 12- dish and pillar structure, 13- palaeocurrent
6 measurements), 14- slumps, Fm: Formation